

# Influence of next-nearest-neighbor electron hopping on the static and dynamical properties of the 2D Hubbard model

Daniel Duffy and Adriana Moreo

Department of Physics, National High Magnetic Field Lab and MARTECH, Florida State University, Tallahassee, FL 32306, USA

(April 15, 2021)

Comparing experimental data for high temperature cuprate superconductors with numerical results for electronic models, it is becoming apparent that a hopping along the plaquette diagonals has to be included to obtain a quantitative agreement. According to recent estimations the value of the diagonal hopping  $t'$  appears to be material dependent. However, the values for  $t'$  discussed in the literature were obtained comparing theoretical results in the weak coupling limit with experimental photoemission data and band structure calculations. The goal of this paper is to study how  $t'$  gets renormalized as the interaction between electrons,  $U$ , increases. For this purpose, the effect of adding a bare diagonal hopping  $t'$  to the fully interacting two dimensional Hubbard model Hamiltonian is investigated using numerical techniques. Positive and negative values of  $t'$  are analyzed. Spin-spin correlations,  $n(\mathbf{k})$ ,  $\langle n \rangle$  vs  $\mu$ , and local magnetic moments are studied for values of  $U/t$  ranging from 0 to 6, and as a function of the electronic density. The influence of the diagonal hopping in the spectral function  $A(\mathbf{k}, \omega)$  is also discussed, and the changes in the gap present in the density of states at half-filling are studied. We introduce a new criterion to determine probable locations of Fermi surfaces at zero temperature from  $n(\mathbf{k})$  data obtained at finite temperature. It appears that hole pockets at  $\mathbf{k} = (\pi/2, \pi/2)$  may be induced for negative  $t'$  while a positive  $t'$  produces similar features at  $\mathbf{k} = (\pi, 0)$  and  $(0, \pi)$ . Comparisons with the standard 2D Hubbard ( $t' = 0$ ) model indicate that a negative  $t'$  hopping amplitude appears to be dynamically generated. In general, we conclude that it is very dangerous to extract a bare parameter of the Hamiltonian ( $t'$ ) from PES data where renormalized parameters play the important role.

## I. INTRODUCTION

As experimental measurements of the properties of high temperature superconducting materials become more accurate, it has been observed that different cuprate compounds present slightly different properties. Among these qualitative differences are the presence of incommensurate magnetic correlations, the symmetry of the pairing state, shape of the Fermi surface (FS), as well as the behavior of the resistivity with temperature.

Many models proposed to describe the cuprate superconductors are particle-hole symmetric and this makes

it impossible to distinguish between electron and hole doped materials. The addition of a diagonal hopping term to the one band Hubbard model has often been suggested as a way to handle the different properties between electron and hole-doped materials since such a term breaks particle-hole symmetry. Even restricted to the family of hole doped materials the inclusion of a diagonal hopping has also been proposed in order to reproduce experimental photoemission (PES) data and band structure calculations. According to these estimations, the diagonal hopping parameter  $t'$  seems material dependent and some of the suggested values are  $t' = 0.20$  for  $Nd_2CeCuO_4$ ,  $t' = -0.20$  for  $La_2SrCuO_4$ , and  $-0.45$  for  $YBa_2Cu_3O_7$ . [1]

Recently, the effect of this  $t'$  hopping term has been analyzed in the weak coupling limit for the Hubbard model [2,3] as well as for the t-J model. [4,5] It was reported that the Fermi surface of the  $U - t - t'$  model in the non-interacting case is in agreement with experimental measurements for appropriate values of  $t'$ , while the FS of the  $t' = 0$  model is not. The same occurs for the magnetic susceptibility and the sign change of the Hall coefficient with doping. [2] However, it is not clear how a moderate or strong Coulombic interaction will modify the properties of weakly interacting electrons. In other words, it is not correct to deduce the value of a *bare* parameter in a Hamiltonian using data from experiments where the *renormalized* parameter plays the key role. It is well known that strong correlations are fundamental in high  $T_c$  models, thus it is likely that the bare  $t'$  is quite different from the renormalized one.

In this paper, we investigate the  $U - t - t'$  model in the intermediate coupling regime using quantum Monte Carlo techniques. We will compare the results with mean field calculations, as well as with the non-interacting limit and with experimental results. The paper is organized as follows: in Section II the model is introduced and its symmetry properties are discussed. Spin-spin correlation functions and incommensurability are studied in Section III. Section IV is devoted to the behavior of the density  $\langle n \rangle$  as a function of chemical potential while local magnetic moments are discussed in Section V. Angle resolved photoemission (ARPES) experiments and the shape of the Fermi surface are studied in Section VI. Dynamical properties appear in Section VII and the conclusions are presented in Section VIII. A mean field analysis is discussed in the Appendix.

## II. THE MODEL

The  $U - t - t'$  Hamiltonian is given by

$$H = -t \sum_{\langle \mathbf{ij} \rangle, \sigma} (c_{\mathbf{i}, \sigma}^\dagger c_{\mathbf{j}, \sigma} + \text{h.c.}) - t' \sum_{\langle \mathbf{in} \rangle, \sigma} (c_{\mathbf{i}, \sigma}^\dagger c_{\mathbf{n}, \sigma} + \text{h.c.}) + U \sum_{\mathbf{i}} (n_{\mathbf{i}\uparrow} - 1/2)(n_{\mathbf{i}\downarrow} - 1/2) + \mu \sum_{\mathbf{i}, \sigma} n_{\mathbf{i}\sigma}, \quad (1)$$

where  $c_{\mathbf{i}, \sigma}^\dagger$  creates an electron at site  $\mathbf{i}$  with spin projection  $\sigma$ ,  $n_{\mathbf{i}\sigma}$  is the number operator, the sum  $\langle \mathbf{ij} \rangle$  runs over pairs of nearest neighbor lattice sites, and the sum  $\langle \mathbf{in} \rangle$  runs over pairs of lattice sites along the plaquette diagonals.  $U$  is the on site Coulombic repulsion,  $t$  the nearest neighbor hopping amplitude,  $t'$  the diagonal hopping amplitude, and  $\mu$  is the chemical potential.

When  $t' = 0$  the above Hamiltonian is particle-hole symmetric, i.e., it remains invariant after the particle-hole transformation operation

$$c_{\mathbf{i}, \sigma}^\dagger \rightarrow (-1)^{\mathbf{i}} c_{\mathbf{i}, \sigma}. \quad (2)$$

If  $t' > 0$  the above transformation maps the Hamiltonian in its particle-hole symmetric one but with  $t' < 0$ , and vice versa. This means that the results obtained for negative (positive)  $t'$  below half-filling can be obtained from the results for positive (negative)  $t'$  above half-filling. In fact, this is the reason why to mimic the effect of electron and hole doping in the  $t$ - $J$  model, (which cannot be doped above half-filling) both signs of  $t'$  are studied below half-filling. [4,5] Then, it is clear that results above and below  $\langle n \rangle = 1$  with different signs for  $t'$  are redundant and in this paper we will study the Hamiltonian (Eq.(1)) only below half-filling with positive and negative values for  $t'$ . We will set  $t = 1$  and  $|t'| = 0.2$  unless stated otherwise.

## III. MAGNETIC CORRELATIONS AND INCOMMENSURABILITY

A spin density wave (SDW) mean field analysis (see Appendix) of the  $U - t - t'$  model predicts the existence of antiferromagnetism at half-filling for  $U > U_c$ . [6] At  $|t'| = 0.2$  it can be shown that  $U_c = 2.1$ . Thus, within the SDW mean field, adding a  $t'$  term appears to decrease the strength of the spin-spin correlations. This result is not unexpected if we consider the large  $U$  limit. In this case a Heisenberg spin-spin interaction with  $J = 4t^2/U$  appears between nearest neighbors sites and a  $J' = 4t'^2/U$  is generated along the diagonals. The  $J'$  interaction introduces frustration and tends to decrease the tendency to antiferromagnetism. In Fig.1-a we present quantum Monte Carlo (QMC) results for the spin-spin correlations  $C(\mathbf{r}) = \langle S_{\mathbf{i}}^z S_{\mathbf{i}+\mathbf{r}}^z \rangle (-1)^{|\mathbf{r}|}$  as a function of distance, at half-filling, for  $U/t = 4$ ,  $t' = 0$  and  $-0.2$  on an  $8 \times 8$  lattice

at  $\beta t = 6$ . Clearly, in both cases there is long range order (or, better, a correlation larger than the system size) but the strength of the antiferromagnetic correlations decreases when  $|t'|$  increases. This is true for either sign of  $t'$  since due to the symmetry of the Hamiltonian at  $\langle n \rangle = 1$  the spin-spin correlations must be the same for both signs of  $t'$ . A similar effect is observed in Fig.1-b as  $U/t$  is increased to 6 at  $\beta t = 4$ .

Previous quantum Monte Carlo calculations on the 2D Hubbard model have indicated that short range incommensurate magnetic correlations develop as the system is doped away from half-filling. [7,8] After these results were reported, neutron scattering experiments revealed short range magnetic incommensuration in  $La_{2-x}Sr_xCuO_4$  (LSCO). [9] The qualitative agreement between theory and experiment was remarkable. However, at a fixed doping, the experimental peaks in the structure factor  $S(\mathbf{k})$  appeared shifted away from  $\mathbf{k} = (\pi, \pi)$  by an amount larger than theoretically predicted. Additional confusion arose when experiments were performed in other materials. It was found that  $Nd_{2-x}Ce_xCuO_4$  does not show incommensurability [10] while for  $YBa_2Cu_3O_{6+x}$  (YBCO) the result is unclear. [11] Several authors suggested that the addition of a material dependent  $t'$  term to the Hubbard Hamiltonian could explain the quantitative, as well as the qualitative, differences observed. All previous studies of the  $U - t - t'$  model have been carried out in the weak coupling limit ( $U/t \leq 4$ ). There are some disagreements among the published results. Bénard et al. [2,12] concentrated on negative values of  $t'$  and used a perturbative approach. They found that incommensurability starts developing at a finite hole density which increases from half-filling as  $t'$  becomes more negative. A similar result, within RPA, was obtained in Ref. [3] though these authors expect incommensurability to disappear for  $t' = -0.45$  due to a decreasing intensity of the peaks in the spectral function. Furukawa and Imada [13] studied positive values of  $t'$  using a zero temperature Monte Carlo algorithm for  $U/t = 4$  and  $t' = 0.25$ . They found incommensurability, but with the peaks in  $S(\mathbf{k})$  moving along the diagonals in the Brillouin zone rather than towards the points  $X = (\pi, 0)$  and  $Y = (0, \pi)$  as found in the experiment and as it happens for  $t' = 0$ . [7,8] Gooding et al. [5] performed exact diagonalization studies of the  $t - t' - J$  model that should resemble the strong coupling limit of the  $U - t - t'$  model. To increase the number of available momenta along particular directions in momentum space they did not use square clusters. For negative values of  $t'$  they observed incommensurability with  $S(\mathbf{k})$  moving along the diagonals, while for positive values of  $t'$  the peak in  $S(\mathbf{k})$  remained at  $(\pi, \pi)$  for all the dopings they studied.

Due to the disparity of all these results and to the lack of numerical data on large square lattices at more realistic couplings larger than  $U/t = 4$ , we decided to carry out a systematic study of the structure factor at  $U/t = 6$  on  $8 \times 8$  lattices using quantum Monte Carlo. We worked at a temperature  $T/t = 1/4$  since due to sign problems it is

not possible to study lower temperatures away from half-filling. Our results are presented in Fig.2 where we show  $S(\mathbf{k})$  along the directions  $(0,0) - (\pi,0) - (\pi,\pi) - (0,0)$  (or  $\Gamma - X - M - \Gamma$ ) for  $U/t = 6$  at different fillings and for positive and negative values of  $t'$ . At half-filling,  $S(\mathbf{k})$  is independent of the sign of  $t'$  due to the symmetry in the Hamiltonian described in Sec.II. As the density is reduced to  $\langle n \rangle = 0.9$ , the strength of  $S(\mathbf{k})$  at the peak is slightly smaller for negative  $t'$  (Fig.2-a) than for positive  $t'$  (Fig.2-b). For negative (positive) hopping the maximum in  $S(\mathbf{k})$  starts moving along the lines from  $(\pi,\pi)$  to  $(\pi,0)$  and  $(0,\pi)$  and it reaches  $\mathbf{k} = (\pi, 3\pi/4)$  and  $(3\pi/4, \pi)$  for  $\langle n \rangle = 0.76$  (0.67). The figure clearly shows that the intensity of the peak in  $S(\mathbf{k})$  is drastically reduced as the doping increases. In fact, when incommensurability appears for positive  $t'$  (Fig.2-h) the peak can barely be seen. However, one has to remember that these features could be strongly enhanced as the temperature decreases.

We conclude that negative values of  $t'$  seem to favor incommensurability more than positive values do. For both signs of  $t'$  we found that doping away from half-filling,  $S(\mathbf{k})$  peaks at  $\mathbf{k} = (\pi, k_m\pi)$  and  $(k_m\pi, \pi)$  where  $0 \leq k_m \leq 1$ , i.e. the peak does not move along the diagonal contrary to the results of Ref. [5,13]. In Fig.3 we plot  $k_m$  vs  $\langle n \rangle$  for  $t' = -0.2, 0$  and  $0.2$  and, for comparison, we also show the experimental results for LSCO [9]. It is clear that  $t' > 0 (< 0)$  slightly decreases (enhances) incommensurability in comparison with the  $t' = 0$  case. The results for  $t' = -0.2$  are closer to the experimental data but to reach a better agreement, it appears that larger negative values of  $t'$  should be used ( $t' \approx -0.4$  linearly extrapolating the results at  $t' = 0.2, 0$  and  $-0.2$ ). This is an example where the value of  $t'$  suggested by comparing Fermi surface shapes obtained from band structure calculations with the ones obtained in the non-interacting case ( $t' = -0.2$  for LSCO) does not provide a good fit for magnetic properties.

We have tried to study the case  $t' = -0.45$ , which is the value suggested for YBCO. Due to sign problems, which become worse as  $|t'|$  increases, we have been able to study only the case  $U/t = 4$  and  $T = t/4$  on an  $8 \times 8$  lattice. We found that the onset of incommensurability occurs at lower doping ( $\langle n \rangle \approx 0.8$ ) but the intensity of the peak in the structure factor,  $S(\mathbf{k})$ , decreases and it is very difficult to decide whether incommensurability has developed. This resembles the experimental results for YBCO [11] that do not allow to determine if the peak in  $S(\mathbf{k})$  shifts away from  $(\pi,\pi)$ . The authors of Ref. [3] found a similar behavior. [14]

Previous analytical work [12,3] predicted that  $k_m$  would become different from 1 immediately upon doping for  $t' = 0$  but only when the density reaches a critical value  $\langle n_c \rangle < 1$  for  $t' < 0$ . Since we work on an  $8 \times 8$  lattice we only can detect incommensurability when  $k_m$  jumps from 1 to 0.75 and thus we cannot check the above mentioned behavior. However, we have not observed qualitative differences for the studied values of  $t'$ . Our results

do not support the claims made in Ref. [5] where it was reported that a positive value of  $t'$  does not induce incommensurability. We found that, in this case, a larger hole doping than was studied in Ref. [5] is required to observe the effect but the tendency to incommensurability eventually occurs. One of the reasons for the disagreement maybe the different symmetry of the clusters studied in Ref. [5] that may induce incommensurability along the diagonals rather than towards X and Y as in the square clusters that we studied, and as it has been experimentally observed.

To summarize, in this section we have studied the behavior of the structure factor as a function of doping for positive and negative values of the diagonal hopping  $t'$ . We found that  $t'$  reduces the strength of the antiferromagnetic correlations at half-filling. Away from  $\langle n \rangle = 1$  a negative hopping promotes incommensuration at a lower doping than a positive one. Using  $t' = -0.2$  we did not find good agreement with experimental data for LSCO showing that deducing bare values of  $t'$  based on PES data may be misleading. For  $t' = -0.45$  incommensurability was difficult to observe due to the strong reduction in the intensity of the peak in the structure factor. This behavior resembles experimental results for YBCO.

#### IV. DENSITY VERSUS CHEMICAL POTENTIAL

A very important property of the Hubbard model is the antiferromagnetic gap that appears at half-filling. This gap can be observed in the density of states by studying the spectral function  $A(\mathbf{k}, \omega)$  (see Sec.VII) or by analyzing the behavior of the density  $\langle n \rangle$  vs  $\mu$ , where  $\mu$  is the chemical potential. It has been found that to change the doping from holes to electrons,  $\mu$  has to cross the gap and a plateau at  $\langle n \rangle = 1$  appears in the  $\langle n \rangle$  vs  $\mu$  curve. [7,15] Since the gap increases with  $U$ , so does the size of the plateau. In this Section we will study the influence of  $t'$  on these results.

Before describing the numerical data let us discuss the expected behavior in the SDW mean field approximation. We found that for the range of parameters analyzed in this paper, the value of  $\Delta$  that satisfies the mean field equations (see Appendix) changes very little when  $t'$  is introduced. For example, working at  $U/t=4$ ,  $\Delta$  is 1.37 for  $|t'| = 0.2$ , i.e. only slightly smaller than at  $t' = 0$  where it takes the value 1.38. However, the main effect of  $t'$  is in a distortion of the bands in such a way that the actual gap in the density of states (DOS) is smaller than  $\Delta$ . For the values of  $t'$  studied, this effect is important only when  $\Delta$  is small.

In Fig.4 we show the mean field energy bands along  $\Gamma - M - X - \Gamma$  in momentum space, for  $t' = 0$  and  $-0.2$  and different values of  $\Delta$  [16]. In Fig.4-a the bands for  $U/t = 6$  are shown; the gap is equal to  $\Delta$  which is 2.48 and it is defined by the difference of energy between the two bands at  $\mathbf{k} = \Sigma = (\pi/2, \pi/2)$  and  $\mathbf{k} = X = (\pi, 0)$

(actually at  $t' = 0$ , the energies  $E(\mathbf{k})$  are degenerate along the line from  $Y = (0, \pi)$  to  $X$ ). When  $t' = -0.2$  the effective gap has been reduced to 2.08 although  $\Delta$  remains at 2.48, as can be seen in Fig.4-b, and it is then 83% of the  $t' = 0$  value. Now the degeneracy along  $X - Y$  has been removed and the effective gap is defined by  $E(X)$  in the conduction band and  $E(\Sigma)$  in the valence band. Results for  $U/t = 4$  are presented in Fig.4-c and d. In this case the effective gap is reduced from 1.38 to 0.97, being now 70% of the original, when  $t'$  changes from 0 to  $-0.2$ . It is clear that as  $U/t$  decreases the effect of  $t'$  on the size of the gap becomes more important. In Fig.4-e we present results for  $\Delta = 0.5$ . This value is interesting because it is well known [7] that the effective size of the gap is reduced in the weak-coupling case due to quantum fluctuations and this value of  $\Delta$  could provide a more accurate representation of the  $U/t = 4$  numerical data. [7] Note that in this case, when  $t' = -0.2$  the effective gap is very small. Then we would expect to see the plateau in  $\langle n \rangle$  vs  $\mu$  very much reduced. For  $U/t = 6$ , on the other hand, the gap changes only slightly at finite  $|t'| = 0.2$  with respect to its value for  $t' = 0$  (see Fig.4-a and b). Then, as  $U/t$  increases, keeping  $t'$  fixed, our expectation is that the effect of  $t'$  on the size of the gap will become increasingly irrelevant.

Now let us analyze the same problem but using QMC techniques. In Fig.5-a,b,c we present  $\langle n \rangle$  vs  $\mu$  for  $t' = 0$  and  $\pm 0.2$  on an  $8 \times 8$  lattice at  $\beta t = 6$  in the non-interacting case. When  $t'$  is negative (positive), half-filling is achieved for a negative (positive) value of the chemical potential rather than at  $\mu = 0$ . It is clear from the figure that, as we pointed out in Section II, the curve for  $t' = 0.2$  can be obtained from the curve at negative  $t'$  using the prescription  $\langle n \rangle(t', \mu) \rightarrow 2 - \langle n \rangle(-t', -\mu)$  even with interactions present. Then, below we will only present results for  $t' = -0.2$ .

What is the effect of a finite Coulombic repulsion? In Fig.5-d and e we present  $\langle n \rangle$  vs  $\mu$  for  $U/t = 4$  and  $\beta t = 6$  on an  $8 \times 8$  lattice. When  $t' = 0$  (Fig.5-d),  $\langle n \rangle$  has a plateau centered at 1 and it is clear that the chemical potential has to move across the gap to change the doping from electrons to holes. For  $t' = -0.2$  (Fig.5-e) the plateau is much smaller and the type of dopants can be changed from holes to electrons varying the chemical potential by a small amount. This behavior is in agreement with experimental data for the high  $T_c$  cuprates obtained by J. Allen's group [17] who observed that the chemical potential does not move across the gap as the dopants are changed from electrons to holes (although these results have not been yet reproduced using other experimental techniques). One alternative explanation of our numerical results may be that the ground state in this case is paramagnetic and the antiferromagnetic gap does not exist, but as we showed in Section III (Fig.1-a) long range antiferromagnetic order has already developed in our finite cluster for the couplings we used thus this idea is incorrect. The SDW mean field calculation presented in the Appendix allows us to better interpret

the data if we assume that the antiferromagnetic gap for  $U/t = 4$  is smaller than the mean field prediction due to quantum fluctuations. If this is the case, the effective gap almost disappears as it was shown before in Fig.4-f. As the Coulombic repulsion is increased to  $U/t = 6$  the plateau at  $\langle n \rangle = 1$  reappears for  $t' = -0.2$  as can be seen in Fig.5-g. In this case the plateau is similar to the one observed for  $t' = 0$  (Fig.5-f). This behavior is also in agreement with the SDW mean field results. The curves presented in Fig.5 appear to be very smooth and they do not indicate the presence of phase separation in the system.

Summarizing, in this section we studied the behavior of the density of electrons as a function of the chemical potential for positive and negative values of a diagonal hopping  $t'$ . We found that  $t'$  reduces the size of the gap. We also found that in weak coupling ( $U/t \leq 4$ ) and at  $|t'| = 0.2$  the chemical potential does not move across the naive gap of order  $U$  when the dopants change from holes to electrons in agreement with the PES results of Allen et al. [17] At larger  $U/t$ , the effect of  $t'$  becomes less important as observed in previous sections.

## V. LOCAL MAGNETIC MOMENTS AND DOUBLE OCCUPANCY

The square of the magnetic moment per site is related to the probability of double occupancy  $\delta = \langle n_{i\uparrow}n_{i\downarrow} \rangle$  through the expression

$$\langle (m_i^z)^2 \rangle = \langle n \rangle - 2\langle n_{i\uparrow}n_{i\downarrow} \rangle. \quad (3)$$

In the non-interacting case the probability of double occupancy is independent of  $t'$ , and it is given by  $\langle n_{i\uparrow}n_{i\downarrow} \rangle = \langle n \rangle^2/4$ . The effect of the interaction  $U$  is to suppress the probability of double occupancy. [7] In the interacting case  $\langle n_{i\uparrow}n_{i\downarrow} \rangle$  depends on  $t'$ . As it can be seen in Fig.6, a negative  $t'$  decreases  $\delta$  when compared with  $t' = 0$  while a positive value increases it. At half-filling and using the symmetry described in Section II, it can be shown that the probability of double occupancy is independent of the sign of  $t'$ . According to Eq.(3) the mean-square magnetic moment per site will slightly increase for negative  $t'$  and decrease for positive  $t'$ .

## VI. PHOTOEMISSION EXPERIMENTS AND FERMI SURFACE

In the last few years much progress has been made in the development of angle-resolved photoemission (ARPES) techniques and reliable data for the quasiparticle dispersion near optimal doping for  $Bi_2Sr_2CaCu_2O_8$  (Bi2212) and YBCO have been obtained. [18] The study of the quasiparticle peak as a function of energy and momentum provides the shape of the Fermi surface for

the different materials. Until recently, some experiments seemed to provide evidence for large electron-like FS [19] but these results have been lately challenged by Aebi et al. [20] Using a new photoemission technique these authors have reported the presence of a so-called shadow band probably due to antiferromagnetic correlations [21], as well as the existence of features resembling hole pockets [22] in Bi2212 (see Fig.7). ARPES also provides information on the quasiparticle bandwidth which appears to be of the order of a fraction of eV independently of the material. Note that this bandwidth is much smaller than the one predicted by LDA calculations [1] which casts doubts on the practice of selecting values of  $t'$  without properly considering the strong correlations. Flat regions about X and Y have also been found in the hole-quasiparticle dispersion. Recently, Wells et al. [23] reported ARPES measurements on the antiferromagnetic insulator  $Sr_2CuOCl_2$ . This material is very difficult to dope but the behavior of the quasiparticle at half-filling is important as a probe for the microscopic theories for holes in antiferromagnets that have been proposed. The authors of Ref. [23] tried to fit their data with a  $t - J$  model with  $J = 0.125\text{eV}$  and found good agreement for the bandwidth but they could not fit the dispersion along the X-Y line. In a recent paper Nazarenko et al. [24] suggested that the addition to the  $t - J$  model of a  $t'$  hopping, which would be material dependent, could help to improve the fitting. Using the Born approximation they obtained agreement with experiments along the X-Y line introducing a  $t' = -0.35t$ , with  $J/t = 0.3$  and  $J = 0.125\text{ eV}$ . Along the  $X - \Gamma$  line disagreement with the experimental data remained although along this line a quasiparticle peak in the experiment is not clearly observed and the error bars are very large. Using the SDW mean field approximation described in the Appendix we calculated the dispersion and we tried to fit the experimental data. Using  $U/t=10$  and  $t' = -0.2t$  we found reasonable agreement with the experimental result as can be seen in Fig.8. These results confirm the importance of  $t'$  terms to describe the cuprates.

As it was stated in the Introduction, one of the reasons often invoked to introduce a  $t'$  hopping in models for high  $T_c$  superconductors is to match the shape of the Fermi surface to experimental results or to LDA calculations. [4] The non-interacting Hubbard model has a nested Fermi surface (FS) at half-filling and it becomes large and electron-like immediately upon doping. The addition of a negative  $t'$  removes the nesting at half-filling and, instead, the FS becomes open and hole-like. Upon further doping it eventually closes but it retains hole-like characteristics. It becomes electron-like only when the hole doping has been further increased. [2] However, it is possible that the introduction of electronic interactions could modify substantially the non-interacting FS. For example, in the two dimensional Hubbard model, the uniform magnetic susceptibility always decreases upon doping in the non-interacting case, but it increases when interactions are strong enough [25] (in agreement with ex-

perimental results). Thus, it is very important to study how interactions affect the shape of the FS.

Since we work on finite lattices it is difficult to accurately determine the FS of a model. Ideally, the FS should be obtained examining the spectral function  $A(\mathbf{k}, \omega)$ . However, as we show in Section VII presently the spectral functions cannot be calculated with enough accuracy and alternative ways of determining the FS must be considered. In some previous papers [7,26] the FS was obtained by calculating the position of the momenta where  $n(\mathbf{k}) \approx 0.5$ . This approach works well for weakly interacting systems, but it may cause problems when strong interactions are considered. One can imagine that for a system with a “hole pocket” centered at  $\Sigma = (\pi/2, \pi/2)$ ,  $n(\mathbf{k})$  along the  $(0, 0) - (\pi, \pi)$  line will jump from a value larger than 0.5 to zero as the pocket is encountered increasing the momentum away from  $(0, 0)$ , defining a first Fermi surface, and then, at the second FS, it will increase again but to some value smaller than 0.5. Then the  $n(\mathbf{k}) \approx 0.5$  criterion is clearly incomplete in strong coupling because it may miss important structure. We can avoid this problem by assuming that a FS is likely to exist where the numerically obtained  $n(\mathbf{k})$  changes very rapidly. In fact, since experiments actually only detect crossovers in  $n(\mathbf{k})$  it is important to know where they occur in numerical simulations. Thus, a study of the values of  $n(\mathbf{k})$  will shed light on possible changes in the shape of the FS as shown below.

Our mean field analysis predicts strong modifications in  $n(\mathbf{k})$  as  $U/t$  increases at a fixed  $t'$ . In particular, at half-filling, fixed  $t'/t$  and large  $U/t$ ,  $n(\mathbf{k})$  resembles more the  $t' = 0$  case with the same  $U/t$  than the  $t' \neq 0$ ,  $U/t = 0$  case. This can be seen from Eq.(9) in the Appendix. If the gap between the conduction and the valence band is such that at half-filling the conduction band is completely filled and the valence band is empty, then  $n(\mathbf{k})$  is given by the same analytical expression as for the  $t' = 0$  model. Indeed, this is what we have observed with QMC. In Fig.9-a we present  $n(\mathbf{k})$  along the line  $X = (\pi, 0)$  to  $Y = (0, \pi)$ , at half-filling for  $U/t = 0, 4$  and  $6$  and  $t' = -0.2$ . The mean field value along this line agrees with the exact result for  $t' = 0$  ( $n(\mathbf{k}) = 0.5$ ) for the finite values of  $U/t$  studied. It appears that as  $U/t$  increases with respect to  $|t'|/t$ ,  $n(\mathbf{k})$  becomes more and more similar to the  $t' = 0$  case, i.e. the concavity tends to disappear and the curve becomes flatter as  $U/t$  increases which is very different from the non-interacting curve as can be seen in the figure. This result at half-filling is not unexpected since as  $U/t$  increases, double occupancy decreases, the diagonal hopping becomes less relevant and the spin part of the model becomes effectively described by a nearest neighbor only Heisenberg Hamiltonian (since  $J' = 4t'^2/U = 0.04J \ll J$  for  $|t'| = 0.2$ ), i.e. the frustrating  $J'$  term is negligible.

Now let us study what happens away from half-filling. In Fig.9-b, c and d, we present  $n(\mathbf{k})$  for the same parameters as in Fig.9-a but for  $\langle n \rangle = 0.9, 0.8$  and  $0.7$ . We also show the corresponding mean field results (open symbols)

for the interacting case. Mean field results are expected to become less reliable as  $\langle n \rangle$  moves further away from 1 and antiferromagnetic correlations decrease. However, the MC points are always closer to the mean field values than to the non-interacting ones.

For negative  $t'$ , the low temperature mean field analysis predicts the formation of hole pockets upon doping about the  $\Sigma = (\pi/2, \pi/2)$  point. On the other hand, in the non-interacting case the hole-like FS is centered about  $M = (\pi, \pi)$ . In addition, in the mean field approximation at zero temperature there are crossovers in  $n(\mathbf{k})$  denoted by the crosses in Fig.10-a where  $T = 0$  mean field results on a  $100 \times 100$  lattice at  $\langle n \rangle = 0.9$ ,  $t' = -0.2$  and  $U/t = 6$  are presented. The full squares define the actual FS and the crosses signal the points where  $n(\mathbf{k})$  changes the most rapidly. The dotted line indicates the points in momentum space where  $n(\mathbf{k}) = 0.5$ . Notice that Fig.10-a resembles the results obtained by Aebi and collaborators, [20] (see Fig.7) if we identify the points of maximum variation in  $n(\mathbf{k})$  with the experimental FS. As the temperature is increased within the mean field approximation the Fermi surface around the pockets disappears [22] and, instead, rapid crossovers are observed, i.e., the solid squares in Fig.10-a are replaced by crosses. For  $U/t = 6$  the pockets remain observable up to  $T/t \approx 1/8$ . As the temperature increases to  $T/t = 1/4$ , i.e., the value used in our Monte Carlo simulations, it can be seen in Fig.10-b that the pockets about  $\Sigma$  have disappeared and only the lines of crossovers remain. The open squares indicate the points where  $n(\mathbf{k}) = 0.5$ . Then, the  $n(\mathbf{k}) = 0.5$  criterion applied to the MF data would incorrectly indicate a closed FS which does not resemble the actual FS at  $T = 0$  at all! In Fig.10-c we show the FS at  $T = 0$  for the non-interacting system. In this case, there is a jump in  $n(\mathbf{k})$  from 1 to 0 at the FS and the two criteria to determine its position agree. As the temperature increases to  $T = 1/4$ , Fig.10-d, in the non-interacting case, both criteria still agree but a spurious crossover is induced along the direction  $\Gamma - X(Y)$  due to temperature effects. However, this variation of  $n(\mathbf{k})$  is much smaller than along the directions where a FS exists at  $T = 0$ .

With this qualitative discussion in mind let us analyze our QMC results obtained on an  $8 \times 8$  lattice at  $T = t/4$  using  $U/t = 6$  and  $t' = -0.2$ . We will consider a system slightly doped away from half-filling with  $\langle n \rangle = 0.9$ . The open squares in Fig.10-e denote the points where  $n(\mathbf{k}) \approx 0.5$  while the crosses denote the regions of maximum variation of  $n(\mathbf{k})$ . These results are in excellent agreement with the mean field calculation on an  $8 \times 8$  lattice at the same temperature. Also notice that this figure resembles Fig.10-b where mean field results at the same temperature on a  $100 \times 100$  lattice are presented.

Now let us point out the differences with the non-interacting case shown in Fig.10-f which is equivalent to Fig.10-e but with  $U=0$ . Notice that the criterion  $n(\mathbf{k}) \approx 0.5$ , denoted by the open squares, provides a ‘‘Fermi surface’’ identical to the one for the  $U/t = 6$  case (Fig.10-e). However, the position of the maximum vari-

ation of  $n(\mathbf{k})$  (crosses) is remarkably different. [27]

Then, one of the main results of this paper is that for intermediate and large values of the Coulomb interaction it is *incorrect* to assume that the shape of the Fermi surface is similar to the non-interacting one. The criterion of maximum variation of  $n(\mathbf{k})$  does not support such an assumption. In this case, a better agreement is obtained when comparing numerical data with a SDW mean field calculation. According to this mean field approach, hole pockets about  $\Sigma$  should be observed at temperatures as high as  $T/t = 1/8$ . This result is in agreement with experiments for Bi2212 [20]. Unfortunately, for  $U/t = 6$  in the interesting doping regimes ( $0.8 \leq \langle n \rangle \leq 0.9$ ), we are not able to obtain accurate results at temperatures lower than  $T/t = 1/4$  because the average value of the sign of the fermionic determinant becomes very small to directly verify the existence of hole pockets.

As a final comment we want to add that a study of the points where  $n(\mathbf{k})$  varies more rapidly for the  $t' = 0$  Hubbard model provides a result qualitatively similar to the one displayed on Fig.10-e suggesting that a negative  $t'$  term may be dynamically generated. [22] For positive  $t'$  hole pockets appear at  $X$ ,  $Y$  and symmetrical points.

In this section we have measured  $n(\mathbf{k})$  numerically and we studied its behavior finding the points in momentum space where it changes more rapidly. The location of these points for negative values of  $t'$  determines a shape very similar to the one experimentally obtained in Ref. [20] where the Fermi surface of Bi2212 was studied.

## VII. DYNAMICAL PROPERTIES

It is very important to understand how the introduction of  $t'$  affects the spectral function  $A(\mathbf{k}, \omega)$ . To evaluate this quantity we used quantum Monte Carlo and the maximum entropy technique. [28] In Fig.11 we show  $A(\mathbf{k}, \omega)$  for  $U/t = 4$  on an  $8 \times 8$  lattice, at  $T = t/6$ , half-filling, and for  $t' = 0$  (Fig.11-a) and  $-0.2$  (Fig.11-b). At half filling and  $t' = 0$  the chemical potential is located inside the gap.  $A(\mathbf{k}, \omega)$  is the same along the line from  $(0, \pi)$  to  $(\pi, 0)$  in agreement with the SDW mean field result and with the numerical observation showing that  $n(\mathbf{k}) = 0.5$  along this line. The size of the gap agrees with the result displayed in Fig.5-d. When  $t' = -0.20$ , as discussed in Section IV, the gap is reduced and, within the accuracy of the maximum entropy procedure, only a pseudogap is observed (Fig.11-b). This again, is in agreement with the results presented in Fig.5-e and with the SDW mean field calculations. Also notice that the chemical potential does not lie inside the pseudogap. It is clear that the symmetry along  $X - Y$  has been removed.

The study of the spectral function should, ideally, determine the shape of the Fermi surface. This is done by observing the momenta where the quasiparticle peak crosses the chemical potential. The problem that we have observed with this approach is that the quasiparticle peak

has a finite width which is rather large due to lack of accuracy of the maximum entropy technique. In fact, the value of  $\mathbf{k}$  at which the peak starts moving across the chemical potential from the left is very different for the value of  $\mathbf{k}$  when the peak has finally moved completely to the right of the chemical potential, and this introduces large error bars. In Fig.11-c we present the spectral function for  $U/t = 8$ ,  $t'/t = -0.2$  at  $\langle n \rangle = 0.9$  and  $T/t = 1/2$  on an  $8 \times 8$  lattice. Along the direction  $\Gamma - X(Y)$  it can be seen that a broad quasiparticle peak moves across the chemical potential; this would suggest the existence of a Fermi surface in this direction as Aebi et al. [20] found but we cannot determine accurately at what value of the momentum the actual crossing occurs. Along the line  $X(Y) - M$  there are indications that a Fermi surface may exist very close to  $X(Y)$ . These Fermi surfaces would appear in the regions where we detected the largest variations of  $n(\mathbf{k})$  (see Fig.10-e). The determination of the FS through the study of the spectral function was used in Ref. [29] where the Hubbard model with  $U/t = 8$  and  $\langle n \rangle = 0.87$  was studied at  $T/t = 1/2$  on up to  $12 \times 12$  lattices. The conclusion is that, in this case, there is a closed Fermi surface centered at  $\mathbf{k} = (\pi, \pi)$ . In Fig.12 we present the shape of the Fermi surface that we obtained studying the problem on an  $8 \times 8$  lattice and using the criteria described in Section VI. The  $n(\mathbf{k}) \approx 0.5$  criterion (open squares) gives an electron-like Fermi surface closed about  $\mathbf{k} = (0, 0)$  as previously observed in Ref. [7] but we have provided enough evidence that this criterion is not necessarily reliable. The points of rapid crossover in  $n(\mathbf{k})$  (stars) provide two surfaces, similar to the behavior predicted by the SDW mean field (see Appendix and Section VI) and the experimental data of Ref. [20].

In the figure we also plot the results obtained from Fig.1 in Ref. [29]. The full circles indicate the values of  $\mathbf{k}$  where the maximum of the quasi-particle peak crosses the chemical potential and the error bars correspond to the width of the peak. Once the data of Ref. [29] are supplemented by the proper error bars, the results are consistent with those obtained with the maximum variation of  $n(\mathbf{k})$  criterion. However, due to the large error bars it is still not possible to decide whether the Fermi surface is closed about  $\Gamma$  or  $M$ .

In this section we studied how a diagonal hopping  $t'$  added to the Hubbard Hamiltonian affects the behavior of the spectral function  $A(\mathbf{k}, \omega)$ . We observed that in weak coupling ( $U/t=4$ ) the gap that appears at half-filling is reduced in agreement with the results presented in Section IV. We found that the data are not accurate enough to allow the unique determination of the shape of the Fermi surface. However, in the strong coupling regime ( $U/t = 8$ ) away from half-filling, we found indications of a Fermi surface consistent with the one presented in Section VI.

## VIII. CONCLUSIONS

In this paper we analyzed the 2D Hubbard model with a diagonal hopping term in the intermediate coupling regime using Monte Carlo techniques. We observed that a diagonal hopping  $t'$  decreases the strength of spin-spin correlations. A negative diagonal hopping accelerates the onset of incommensurability while a positive one retards it. The intensity of the peak in the structure factor decreases rapidly as the system is doped away from half-filling but its strength may increase at lower temperatures. Comparing our numerical results with experimental data for LSCO, we found that a  $t'$  more negative than the suggested value [1] -0.2 appears to be needed to reach quantitative agreement.

We found that  $t'$  tends to reduce the size of the antiferromagnetic gap but this effect is important only in the weak coupling regime. Double occupancy is enhanced (reduced) by a positive (negative) diagonal hopping. This effect does not occur in the non-interacting case.

A study of  $n(\mathbf{k})$  allows us to define a new criterion to find probable locations of Fermi surfaces working numerically at finite temperature. Since experimentalists also work at finite temperature and find the FS as the points in momentum space where  $n(\mathbf{k})$  has rapid crossovers, we looked at these points in our numerical data. We observed that lines of rapid crossovers in  $n(\mathbf{k})$  appear in positions similar to the FS obtained experimentally at room temperature for Bi2212 [20]. An analogous result is obtained for the  $t' = 0$  case which indicates that a negative hopping term may be dynamically generated.

A study of the spectral functions show how the addition of a diagonal hopping term removes the symmetry along the line  $X - Y$  and reduces the size of the gap at half-filling.

We conclude that it is very dangerous to extract a bare parameter of the Hamiltonian like  $t'$  from experimental (PES) data where renormalized parameters play the important role.

## IX. ACKNOWLEDGMENTS

We thank A. Sandvik for providing his maximum entropy code and E. Dagotto, A. Kampf, Q. Si, A.M. Tremblay and L. Chen for useful conversations and suggestions. This work is supported by the Office of Naval Research under grant ONR N00014-93-0495 and ONR N00014-94-1-1031. We thank SCRI and the Computer Center at FSU for providing us access to their Cray-YMP supercomputer and also ONR for giving us access to their CM5 connection machine.

## X. APPENDIX: SDW MEAN FIELD

The spin density wave (SDW) mean field formalism has been applied to the Hubbard model [30] and also to the  $U-t-t'$  model [6,31]. At half-filling the ground state for the  $U-t-t'$  model is antiferromagnetic if  $U > U_c$ ; the critical coupling  $U_c$  is a function of  $t'$  and for  $|t'| = 0.2$  we found numerically  $U_c \approx 2.5$ . [32] Since we will study  $U=4$  or higher we want to concentrate in the antiferromagnetic solution. In this case we found two energy bands given by

$$E_k^\pm = -4t' \cos k_x \cos k_y - \mu \pm E_k^0, \quad (4)$$

where

$$E_k^0 = \sqrt{\epsilon_k^2 + \Delta^2}, \quad (5)$$

$$\epsilon_k = -2t(\cos k_x + \cos k_y), \quad (6)$$

and  $\Delta$  is obtained by solving the self-consistent equations:

$$\frac{1}{U} = \sum_k \frac{[f(E_k^-) - f(E_k^+)]}{E_k^0}, \quad (7)$$

and

$$\langle n \rangle = \sum_k n(k). \quad (8)$$

where  $f(x)$  is the fermi function given by  $\frac{1}{e^{\beta x} + 1}$  and

$$n(k) = \frac{1}{2} \left(1 - \frac{\epsilon_k}{E_k^0}\right) f(E_k^-) + \frac{1}{2} \left(1 + \frac{\epsilon_k}{E_k^0}\right) f(E_k^+). \quad (9)$$

- 
- [1] W.E. Pickett, Rev. Mod. Phys. **61**, 433, (1989); M.S. Hybertsen, et al., Phys. Rev. B **41**, 11068, (1990); M.S. Hybertsen, et al., Phys. Rev. B **45**, 10032 (1992); J.J. Yu, S. Massida, A.J. Freeman and D.D. Koelbing, Phys. Lett. **A 122**, 203 (1987); L.F. Mattheiss, Phys. Rev. Lett. **58**, 1078, (1987); J. Yu et al. Phys. Rev. Lett. **58**, 1035, (1987).
  - [2] P. Bénard, L. Chen, and A.M. Tremblay, Phys. Rev. B **47**, 15217 (1993).
  - [3] Q. Si, T. Zha, K. Levin and J.P. Lu, Phys. Rev. B **47**, 9055, (1993).
  - [4] T. Tanamoto, K. Kuboki and H. Fukuyama, J. Phys. Soc. Jap. **60**, 3072, (1991); E. Gagliano, S. Bacci and E. Dagotto, Phys. Rev. B **42** 6222 (1990); T. Tokyama and S. Maekawa, Phys. Rev. B **49**, 3596, (1994); M. Lavagna and G. Stemann, Phys. Rev. B **49**, 4235 (1994); G. Stemann, C. Pépin and M. Lavagna, Phys. Rev. B **50**, 4075 (1994).
  - [5] R.J. Gooding, K.J.E. Vos and P.W. Leung, Phys. Rev. B **49**, 4119 (1994); R.J. Gooding, K.J.E. Vos and P.W. Leung, Phys. Rev. B **50**, 12866, (1994).
  - [6] H.Q. Lin and J.E. Hirsch, Phys. Rev. B **35**, 3359 (1987).
  - [7] A. Moreo et al., Phys. Rev. B **41**, 2313 (1990).
  - [8] A. Moreo, E. Dagotto, T. Jolicœur and J. Riera, Phys. Rev. B **42**, 6283, (1990).
  - [9] S.W. Cheong et al., Phys. Rev. Lett. **67**, 1791 (1991).
  - [10] T.R. Thurston, et al., Phys. Rev. Lett. **65**, 263, (1990).
  - [11] J.M. Tranquada, P.M. Gehring, G. Shirane, S. Shamoto and M. Sato, Phys. Rev. B **46**, 5561, (1992).
  - [12] P. Bénard, L. Chen, and A.M. Tremblay, Phys. Rev. B **47**, 589 (1993).
  - [13] N. Furukawa and M. Imada, J. Phys. Soc. Jap. **61**, 3331, (1992).
  - [14] Q. Si, private communication.
  - [15] E. Dagotto et al., Phys. Rev. B **45**, 10741, (1992) and references therein.
  - [16] The results for  $t' = 0.2$  are obtained by exchanging valence and conduction bands.
  - [17] J.W. Allen, et al., Phys. Rev. Lett. **64**, 595 (1990).
  - [18] D.S. Dessau et al., Phys. Rev. Lett. **71**, 2781, (1993); K. Gofron et al., J. Phys. Chem. Solids **54**, 1193, (1993).
  - [19] J.C. Campuzano et al., Phys. Rev. Lett. **64**, 2308 (1990) and Phys. Rev. B **43**, 2788, (1991); Liu Rong et al., Phys. Rev. B **45**, 5614 (1992) and Phys. Rev. B **46**, 11056 (1992).
  - [20] P. Aebi et al., Phys. Rev. Lett. **72**, 2757 (1994).
  - [21] A. Kampf and J.R. Schrieffer, Phys. Rev. B **42**, 7967, (1990); S. Haas, A. Moreo and E. Dagotto, Phys. Rev. Lett. **74**, 4281 (1995).
  - [22] D. Duffy and A. Moreo, Phys. Rev. B **51**, 11882 (1995).
  - [23] B.O. Wells et al., Phys. Rev. Lett. **74**, 964 (1995).
  - [24] A. Nazarenko, K.J.E. Vos, S. Haas, E. Dagotto and R.J. Gooding, Phys. Rev. B **51**, 8676 (1995).
  - [25] A. Moreo, Phys. Rev. B **48**, 3380 (1993).
  - [26] W. Stephan and P. Horsch, Phys. Rev. Lett. **66**, 2258

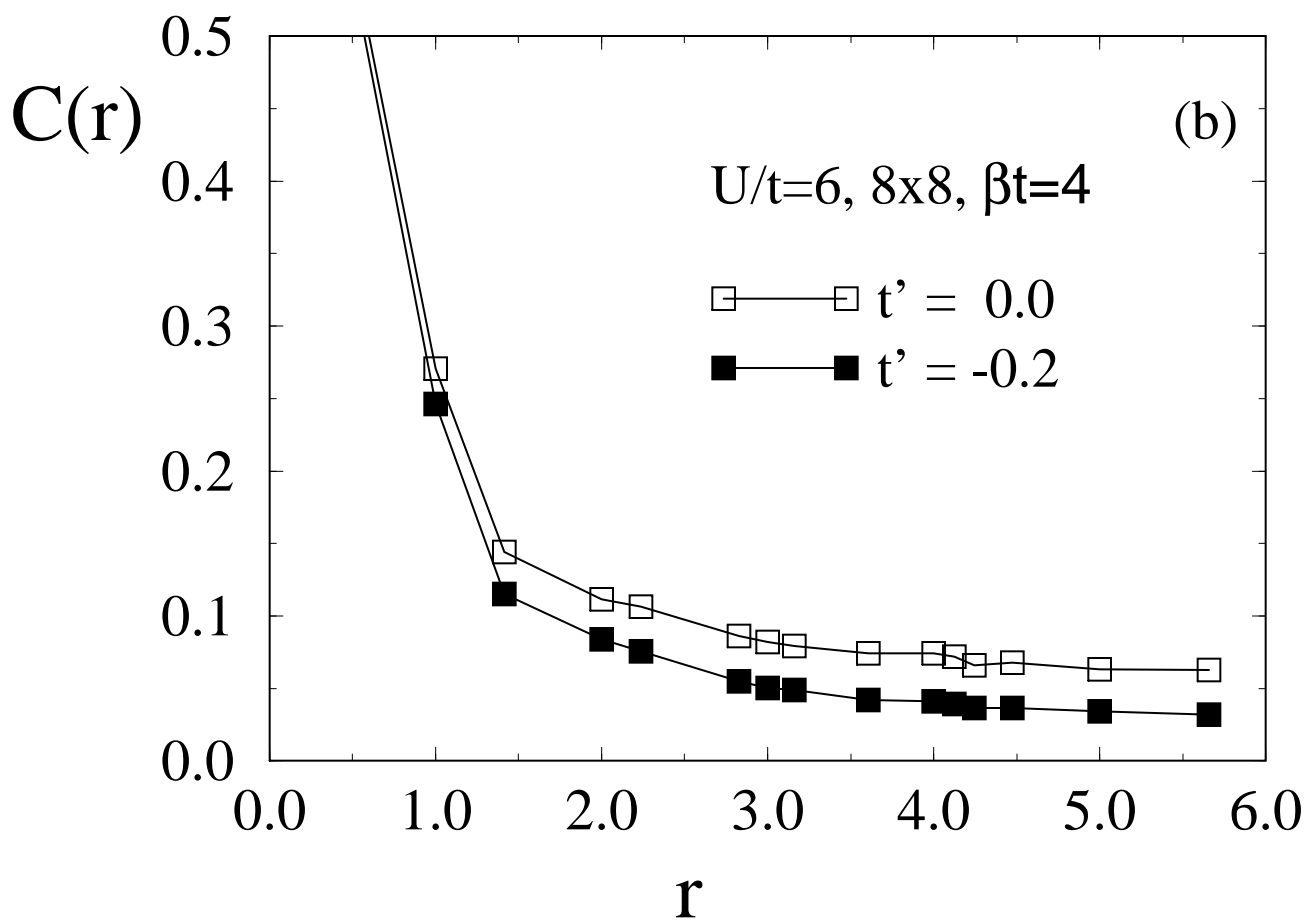
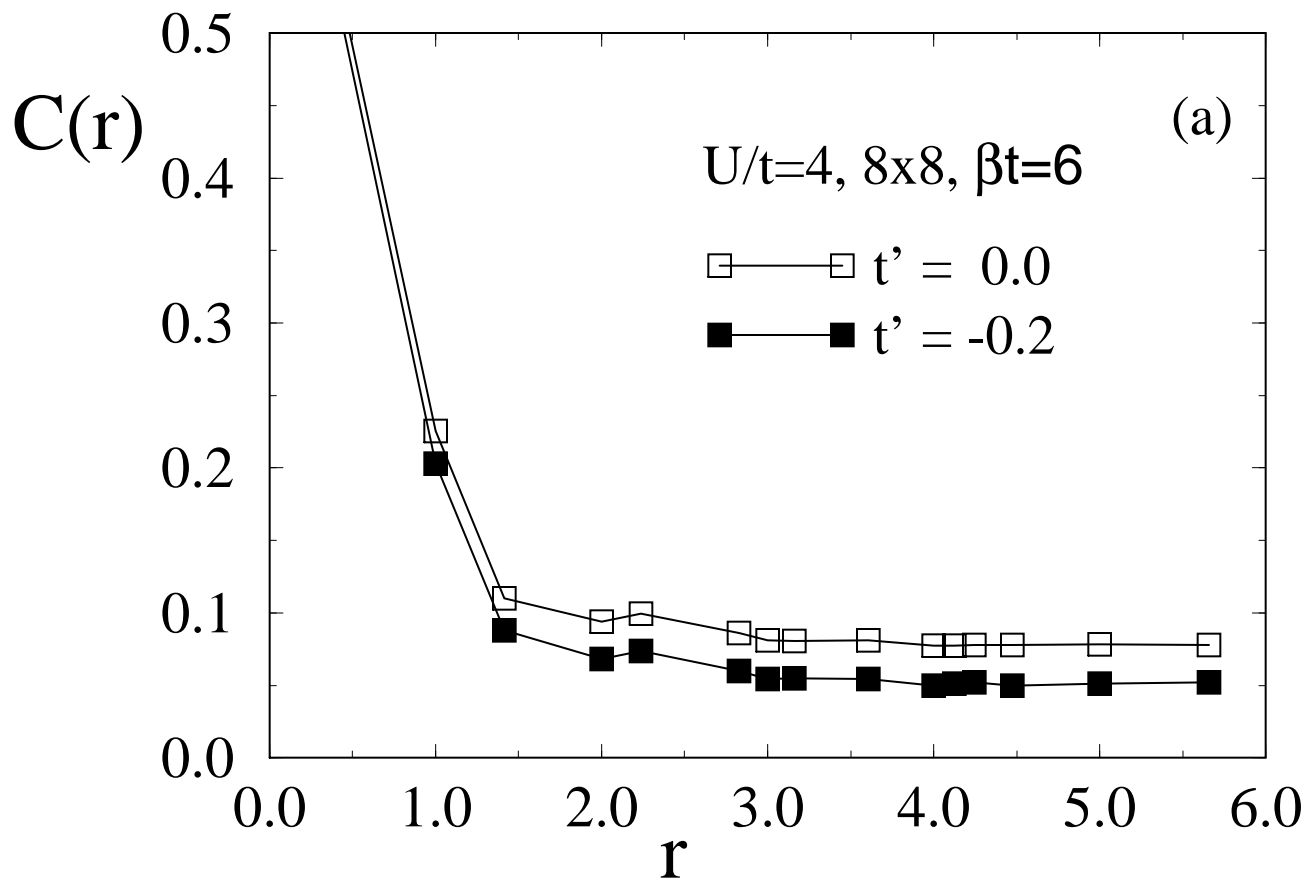


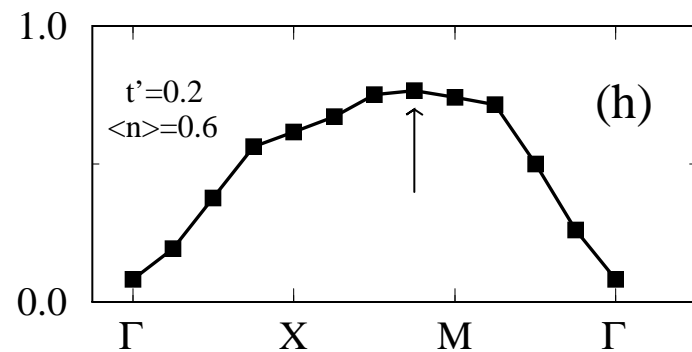
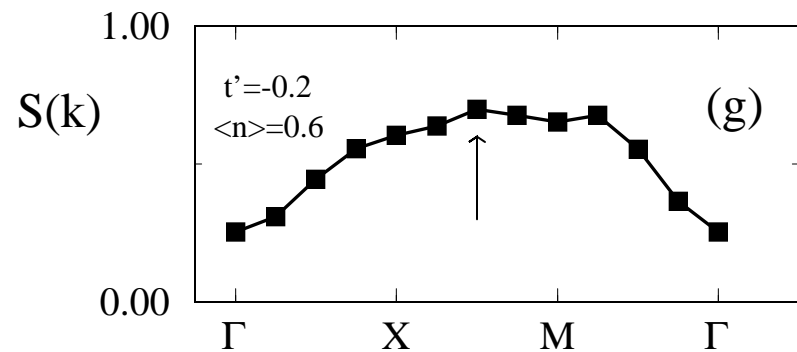
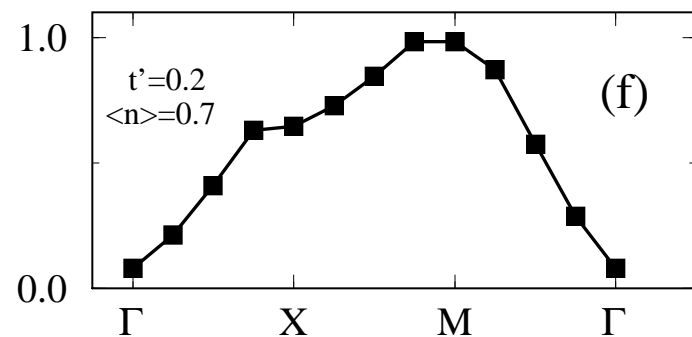
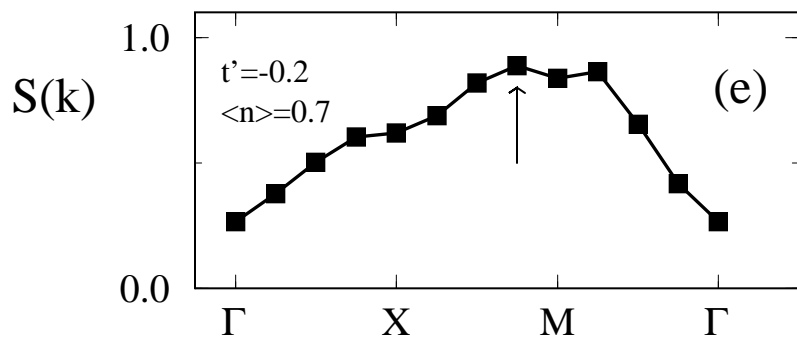
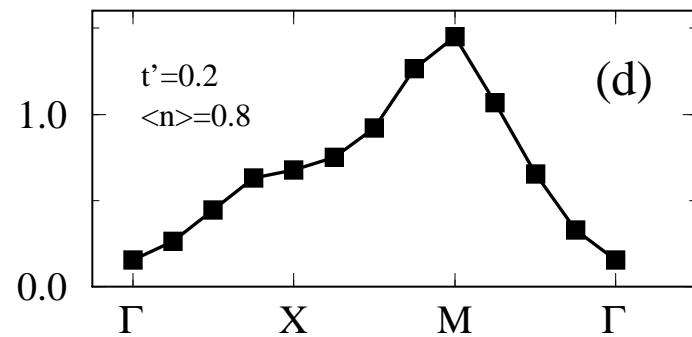
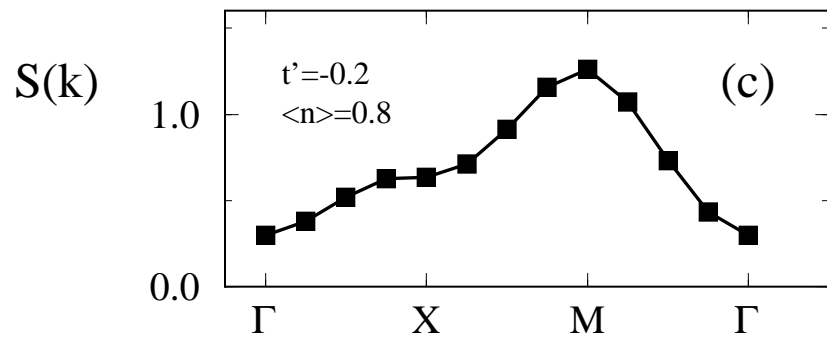
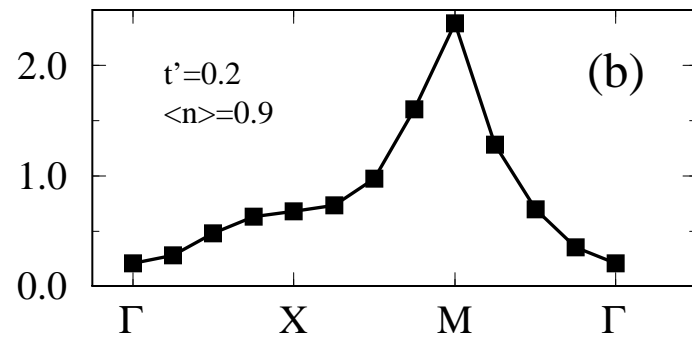
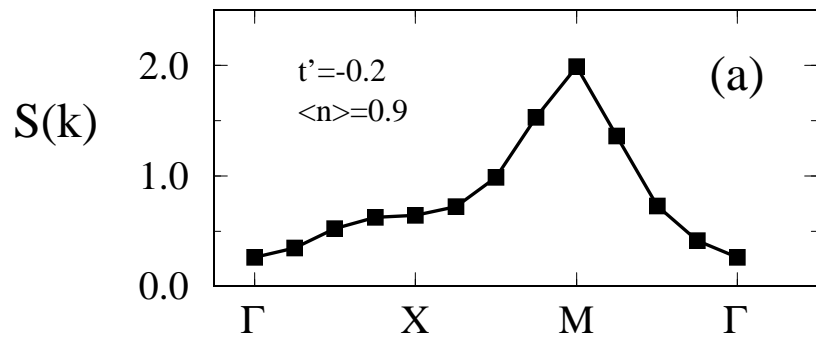
(1991).

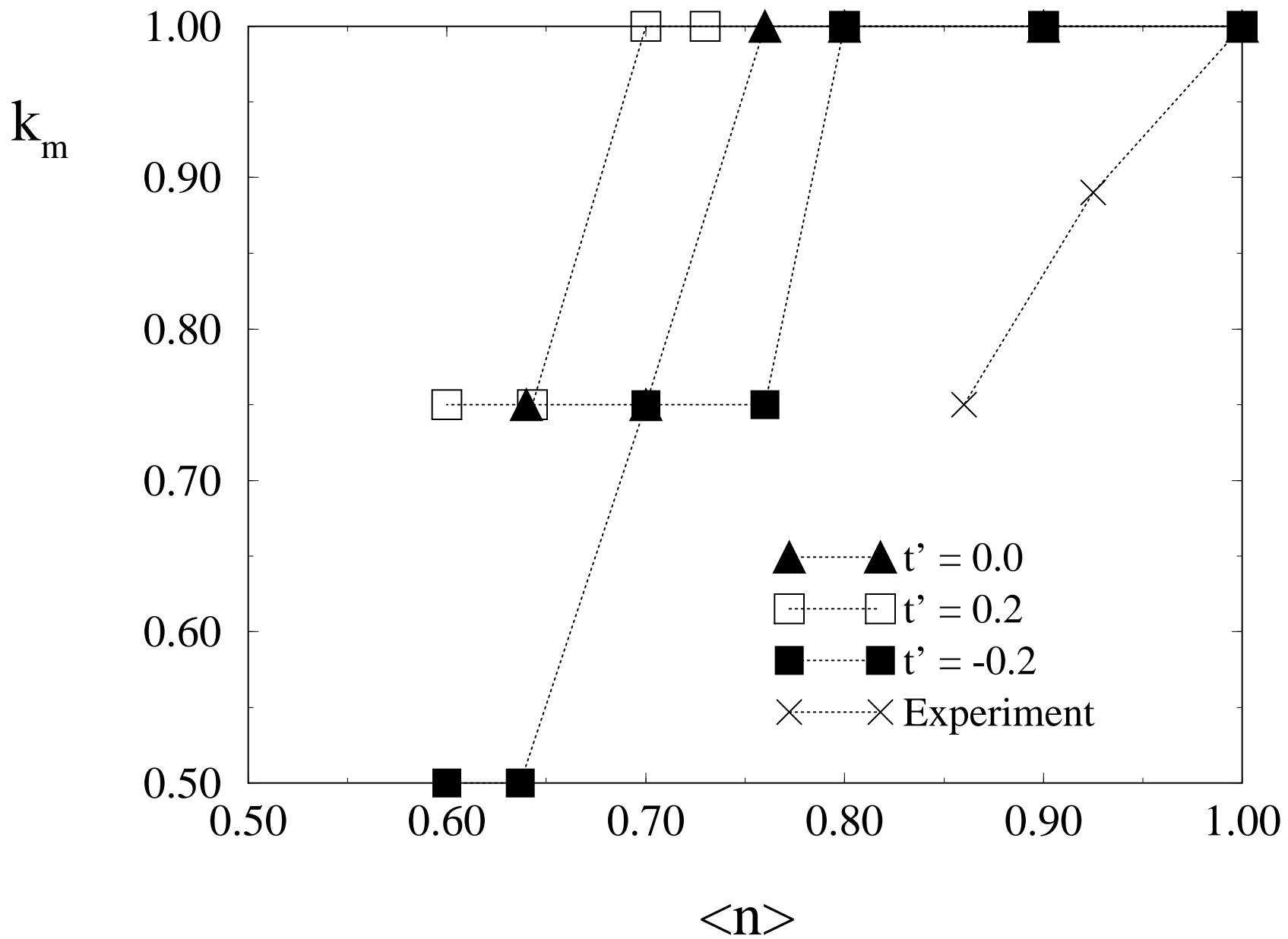
- [27] Notice the resemblance between Fig.10-f and 10-d indicating that finite size effects are not very strong.
- [28] R.N. Silver, D.S. Sivia and J.E. Gubernatis, Phys. Rev. B 41, 2380 (1990).
- [29] N. Bulut, D.J. Scalapino and S.R. White, Phys. Rev. B 50, 7215, (1994).
- [30] J.R. Schrieffer, X.G. Wen and S.C. Zhang, Phys. Rev. B 39, 11663 (1989)
- [31] A. Chubukov and K. Musaelian, Phys. Rev. B 50, 6238, (1994).
- [32] This result is in agreement with the value reported in Ref.6.

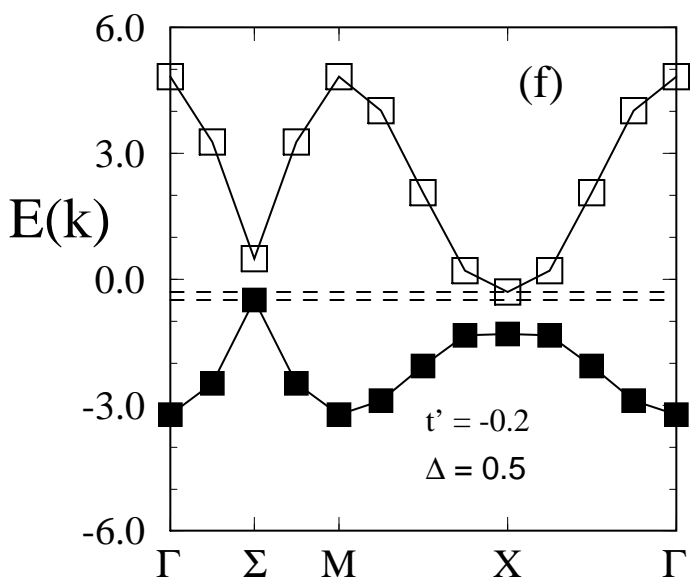
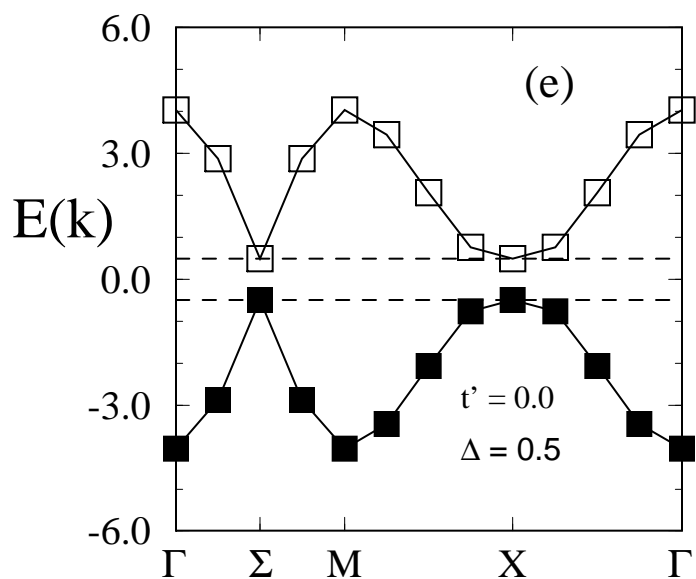
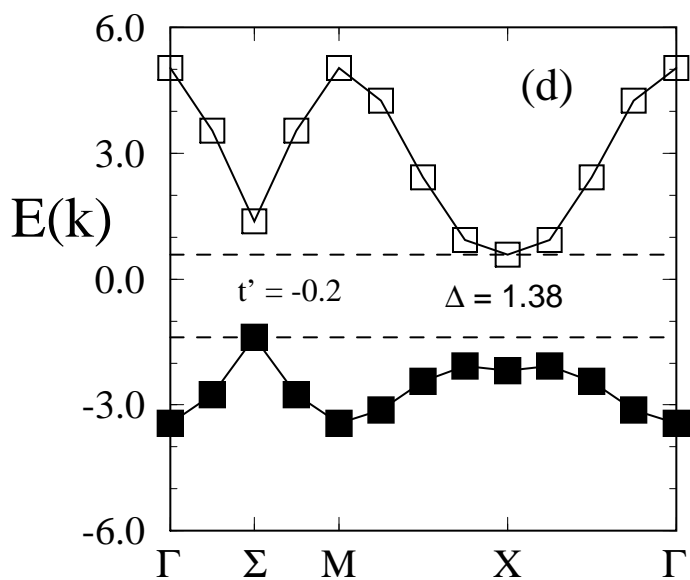
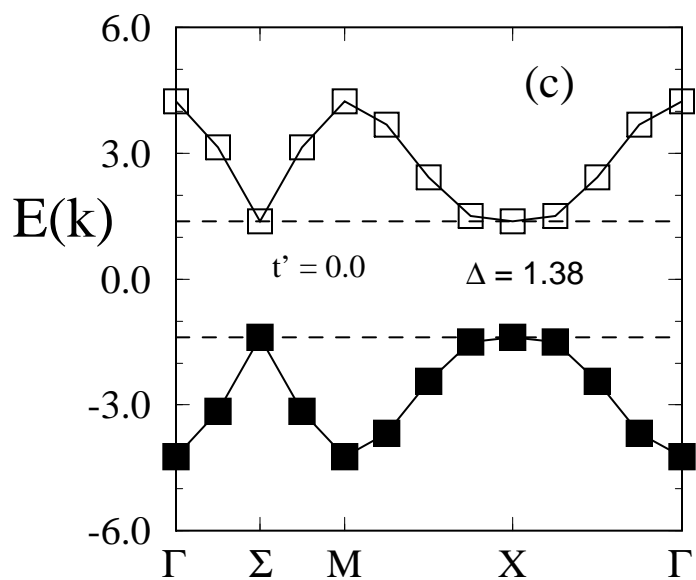
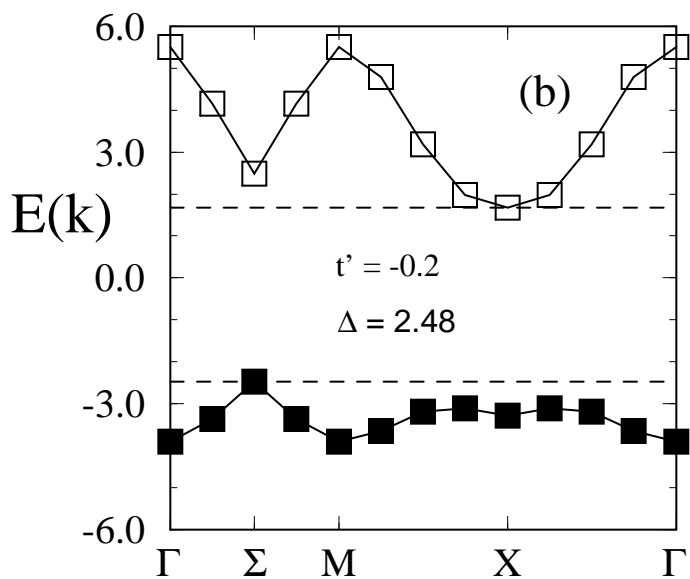
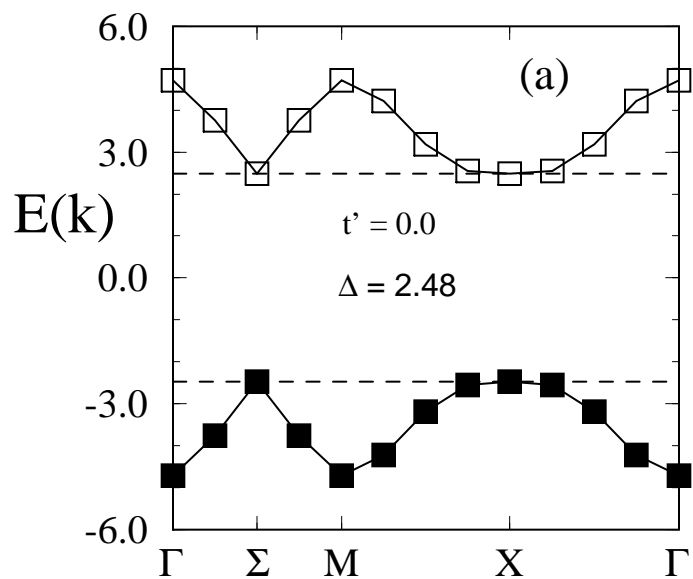
### Figure Captions

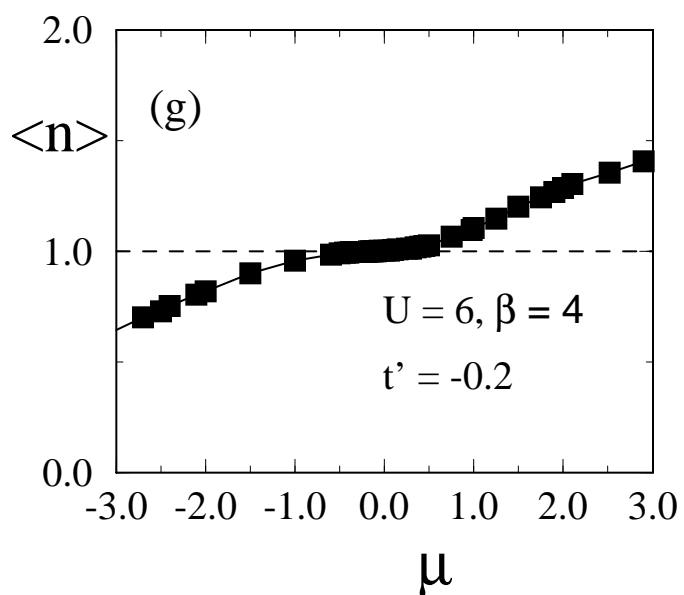
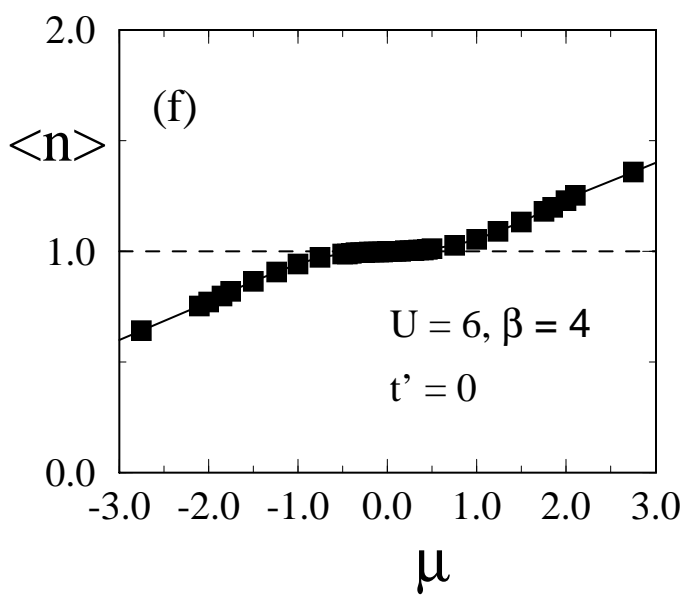
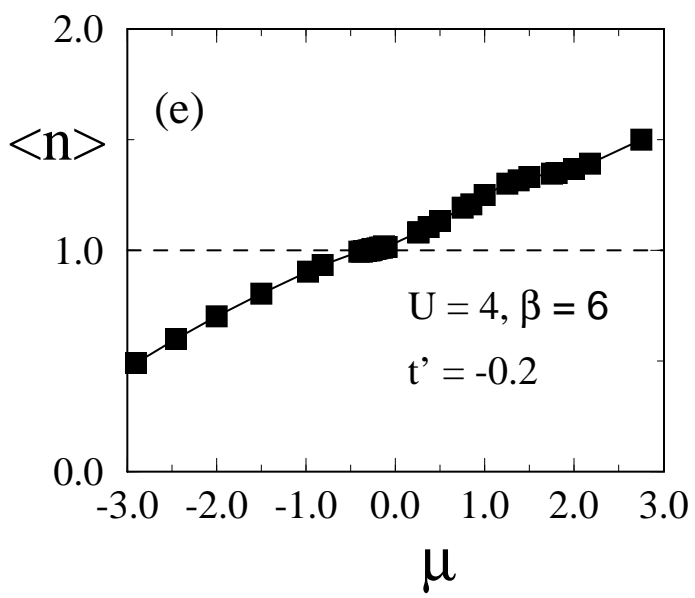
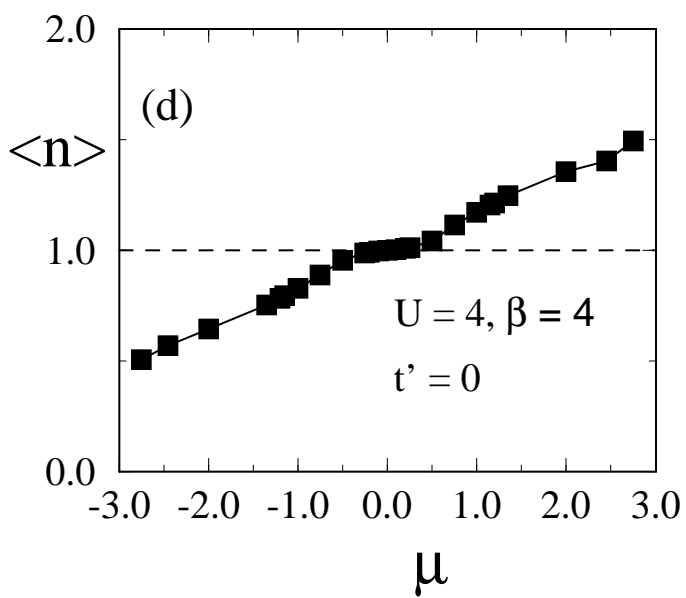
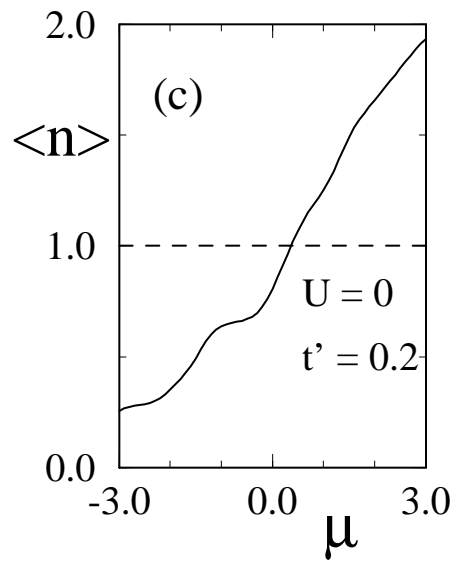
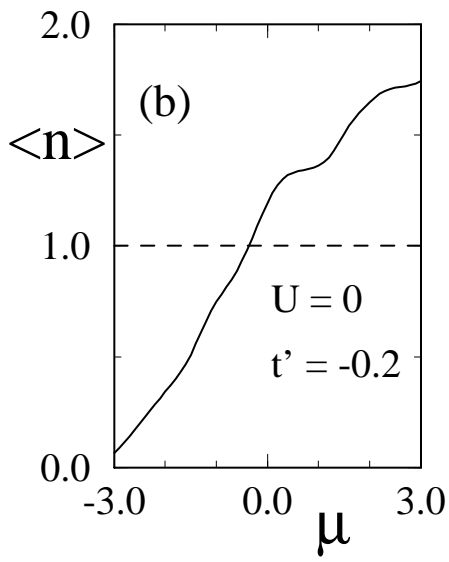
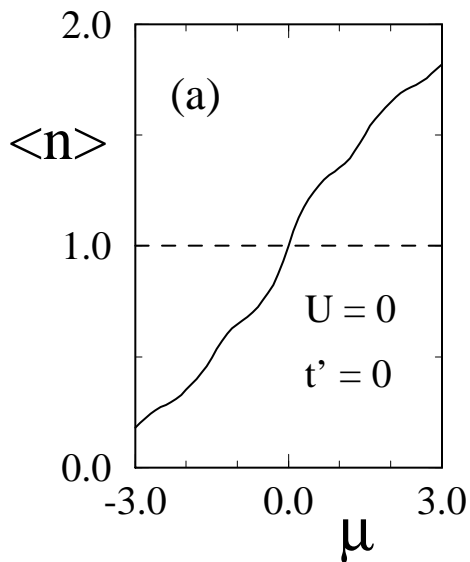
1. (a) Spin-spin correlation  $C(\mathbf{r}) = \langle S_{\mathbf{i}}^z S_{\mathbf{i}+\mathbf{r}}^z \rangle (-1)^{|\mathbf{r}|}$  for  $U/t = 4$ ,  $T = t/6$  on an  $8 \times 8$  lattice at half-filling for  $t' = 0$  (open squares) and  $t' = -0.2$  (filled squares). The error bars are of the size of the dots; (b) Same as (a) for  $U/t = 6$ ,  $T = t/4$ .
2. (a) Structure factor  $S(\mathbf{k})$  along the lines  $\Gamma - X - M - \Gamma$  for  $U/t = 6$  and  $\beta t = 4$  on an  $8 \times 8$  lattice at  $\langle n \rangle = 0.9$  and  $t' = -0.2$ ; (b) Same as (a) for  $t' = 0.2$ ; (c) Same as (a) for  $\langle n \rangle = 0.8$ ; (d) Same as (c) for  $t' = 0.2$ ; (e) Same as (a) for  $\langle n \rangle = 0.7$ ; (f) Same as (e) for  $t' = 0.2$ ; (g) Same as (a) for  $\langle n \rangle = 0.6$ ; (h) Same as (g) for  $t' = 0.2$ .
3. Value of  $k_m$  as a function of doping for  $t' = 0.2$  (open squares), 0 (triangles) and  $-0.2$  (dark squares) for  $U/t = 6$  on an  $8 \times 8$  lattice and  $\beta t = 4$ . The crosses are experimental data from Ref. [9].
4. (a) SDW mean field energy bands on an  $8 \times 8$  lattice along  $\Gamma - M - X - \Gamma$  in momentum space, for  $\Delta = 2.48$  that corresponds to  $U/t = 6$  for  $t' = 0$ ; the effective gap is shown with dashed lines; (b) Same as (a) but for  $t' = -0.2$ ; (c) Same as (a) but for  $\Delta = 1.38$  that corresponds to  $U/t = 4$ . (d) Same as (c) but for  $t' = -0.2$ ; (e) Same as (a) but for  $\Delta = 0.5$ . (f) Same as (e) but for  $t' = -0.2$ .
5. (a) The density  $\langle n \rangle$  as a function of  $\mu$  on an  $8 \times 8$  lattice for  $U/t = 0$ ,  $T = t/6$  and  $t' = 0$ . (b) Same as (a) for  $t' = -0.2$ ; (c) Same as (a) for  $t' = 0.2$ ; (d) Same as (a) for  $U/t = 4$ ; (e) Same as (b) for  $U/t = 4$ ; (f) Same as (a) for  $U/t = 6$  with  $T = t/4$ ; (g) Same as (f) for  $t' = -0.2$ . The error bars are smaller than the symbols.
6. Probability of double occupancy  $\delta$  as a function of filling  $\langle n \rangle$  on an  $8 \times 8$  lattice at  $\beta = 4$  and  $t = 1$  for  $U=6$  and  $t' = 0.2$  (open squares), 0 (crosses) and  $-0.2$  (filled squares). The filled triangles are results for  $U/t=0$ .
7. Fermi surface for Bi2212 as shown in Ref. [20].
8. Quasiparticle dispersion of the  $U - t - t'$  model calculated using a SDW mean field using  $t' = -0.2t$ ,  $U/t = 10$  and  $U = 4\text{eV}$  (solid line),  $t - J$  results (dotted line) and experimental ARPES results from Ref. [23]. Through the relationship  $J = 4t^2/U$  we found  $J/t = 0.4$  and using  $t = 0.4\text{eV}$  we get  $J = 0.16\text{eV}$ .
9. Quantum MC values for  $n(\mathbf{k})$  along  $X - Y$  on an  $8 \times 8$  lattice at  $\beta t = 4$  and  $t' = -0.2$  for  $U = 0$  (crosses),  $U = 4$  (filled circles) and  $U = 6$  (filled squares) and mean field results indicated by open circles ( $U = 4$ ) and open squares ( $U = 6$ ) and connected with dashed lines for a)  $\langle n \rangle = 1.0$  (in this case the MF results along the direction shown are independent of  $U$  and open circles only are used), b)  $\langle n \rangle = 0.9$ , c)  $\langle n \rangle = 0.8$ , and d)  $\langle n \rangle = 0.7$ .
10. a) Mean field results for  $U/t = 6$ ,  $T = 0$  and  $\langle n \rangle = 0.9$  on a  $100 \times 100$  lattice. The dark squares denote the Fermi surface; the crosses indicate the values of  $\mathbf{k}$  where  $n(\mathbf{k})$  changes most rapidly and the dotted line indicates the values of  $\mathbf{k}$  where  $n(\mathbf{k}) = 0.5$ ; b) same as a) for  $T/t = 1/4$ . Here, there is no real Fermi surface and the values of  $\mathbf{k}$  where  $n(\mathbf{k}) = 0.5$  are indicated by open squares; c) same as a) for  $U/t = 0$ ; d) same as b) for  $U/t = 0$ ; e) Monte Carlo results for  $U/t = 6$ ,  $T/t = 1/4$  and  $\langle n \rangle = 0.9$  on a  $8 \times 8$  lattice. The crosses indicate the values of  $\mathbf{k}$  where  $n(\mathbf{k})$  changes most rapidly and the open squares indicate the values of  $\mathbf{k}$  where  $n(\mathbf{k}) = 0.5$ ; f) same as e) for  $U/t = 0$ .
11. a)  $A(\mathbf{k}, \omega)$  for  $U/t = 4$ ,  $t' = 0$ ,  $T/t = 1/6$  on an  $8 \times 8$  lattice at half-filling. The moments are in units of  $\pi/4$ . The dotted line indicates the position of the chemical potential; b) same as a) for  $t' = -0.2$ ; c)  $A(\mathbf{k}, \omega)$  for  $U/t = 8$ ,  $t' = -0.2$ ,  $T/t = 1/2$  on an  $8 \times 8$  lattice at  $\langle n \rangle = 0.9$ .
12. Fermi surface for the 2D Hubbard model with  $U/t = 8$ ,  $\langle n \rangle = 0.87$  at  $T/t = 1/2$  using the  $n(\mathbf{k}) = 0.5$  criterion (open squares and solid line), the maximum variation of  $n(\mathbf{k})$  criterion (stars and dashed line) and from the maximum entropy results of Ref. [29] (solid circles, with error bars, and dotted line).



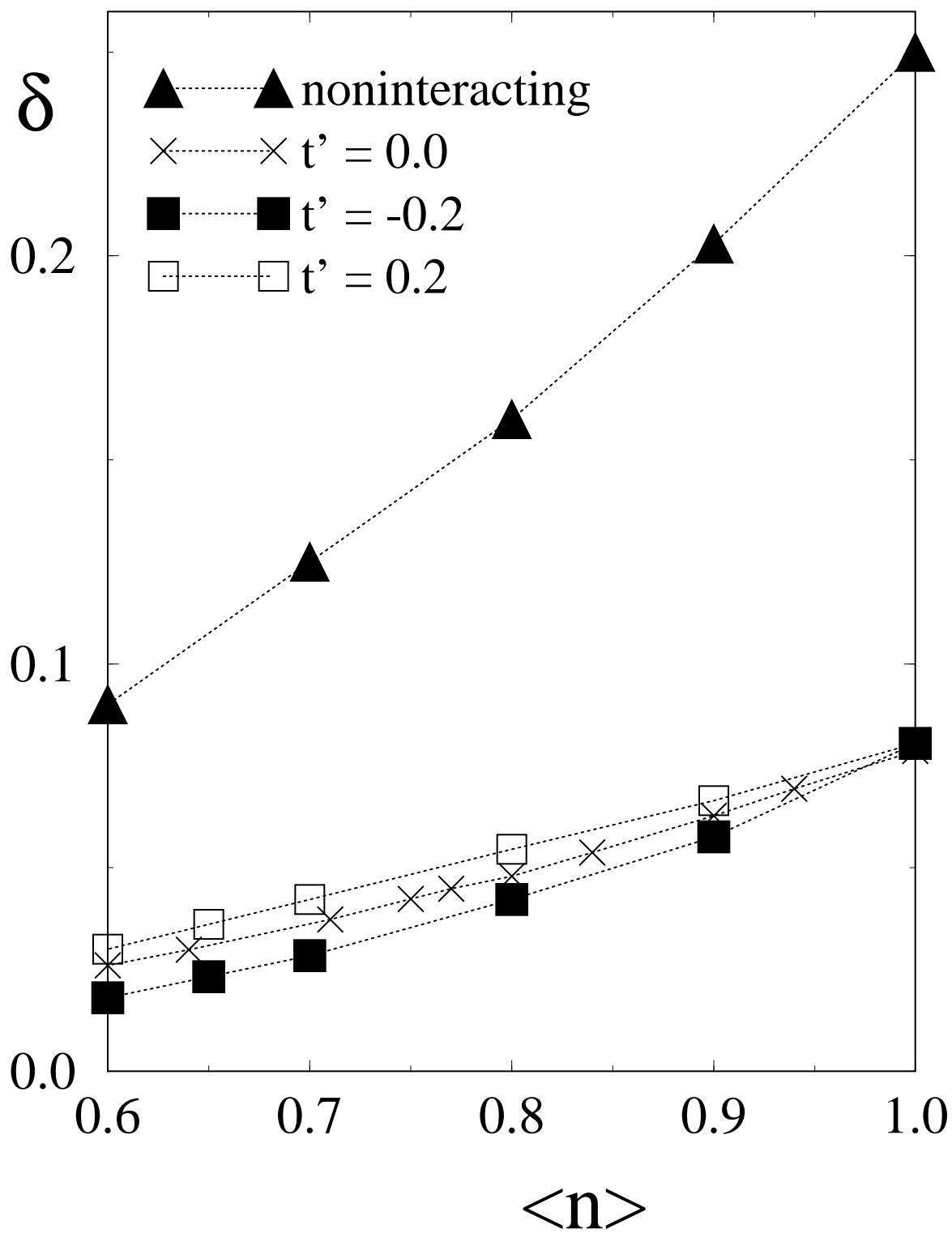


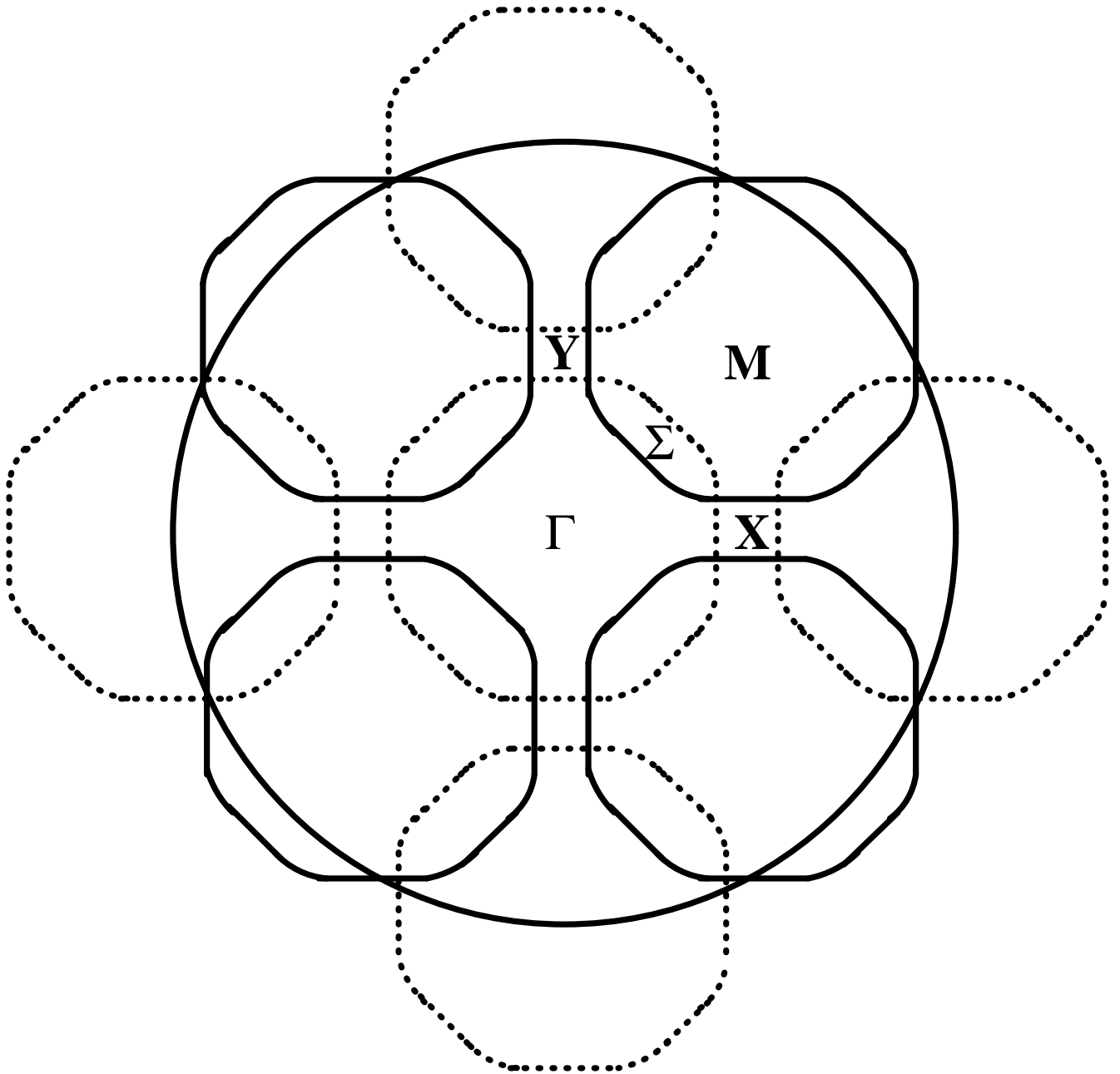




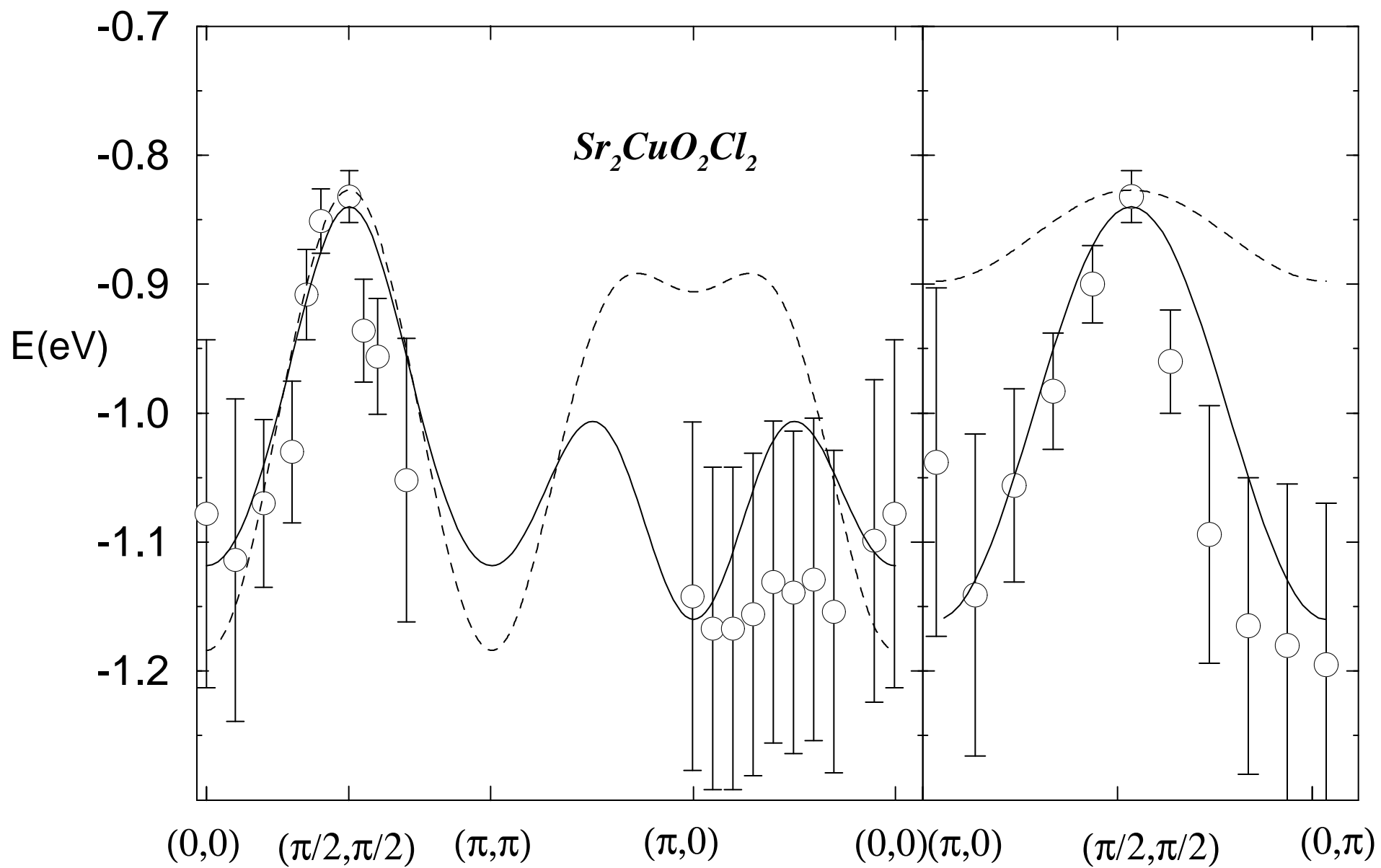


8x8,  $U=6$ ,  $\beta=4$

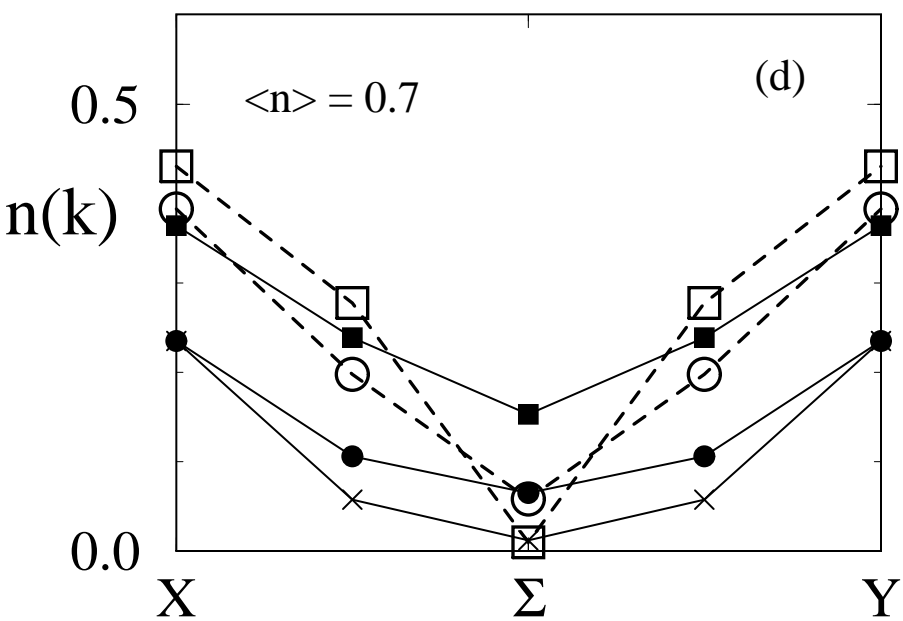
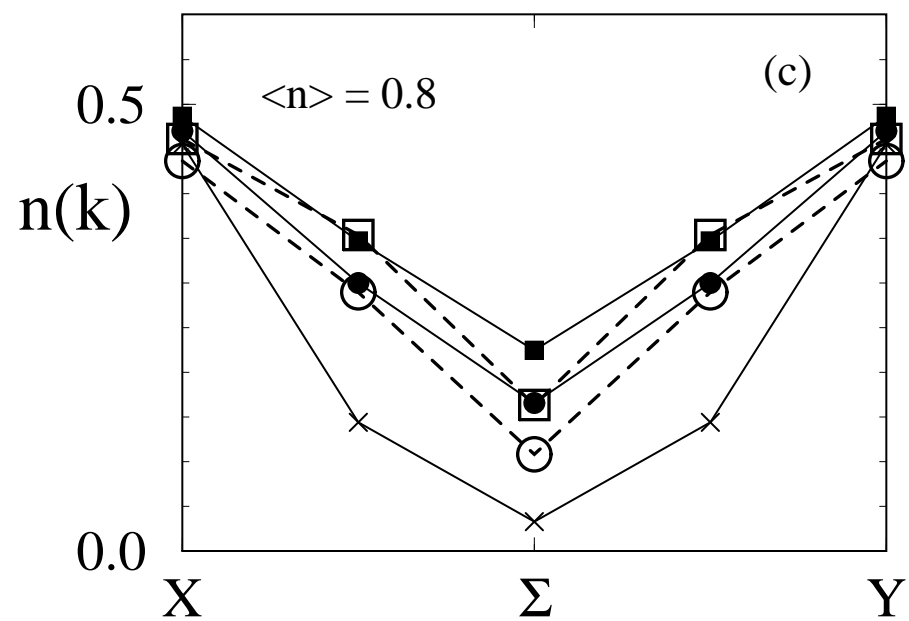
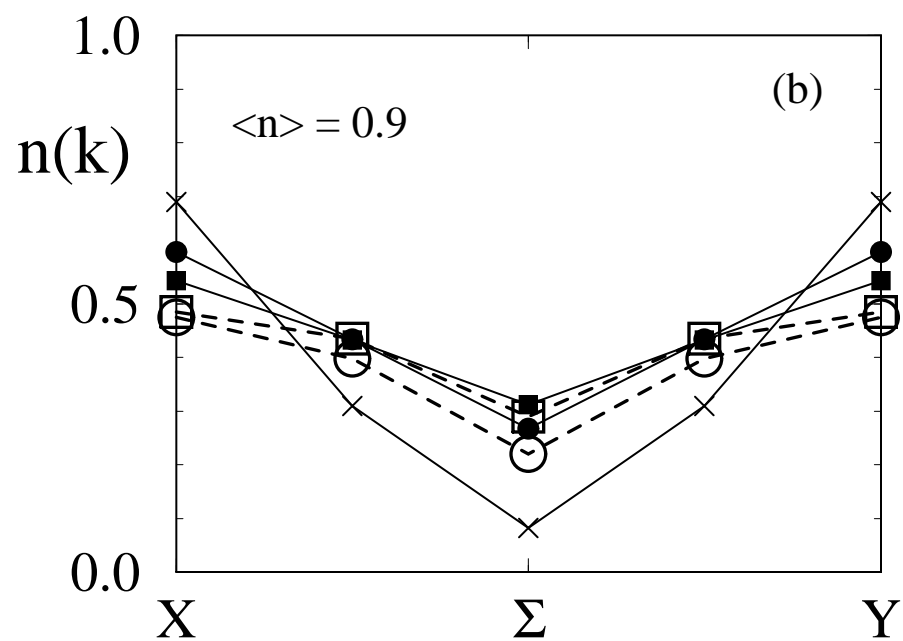
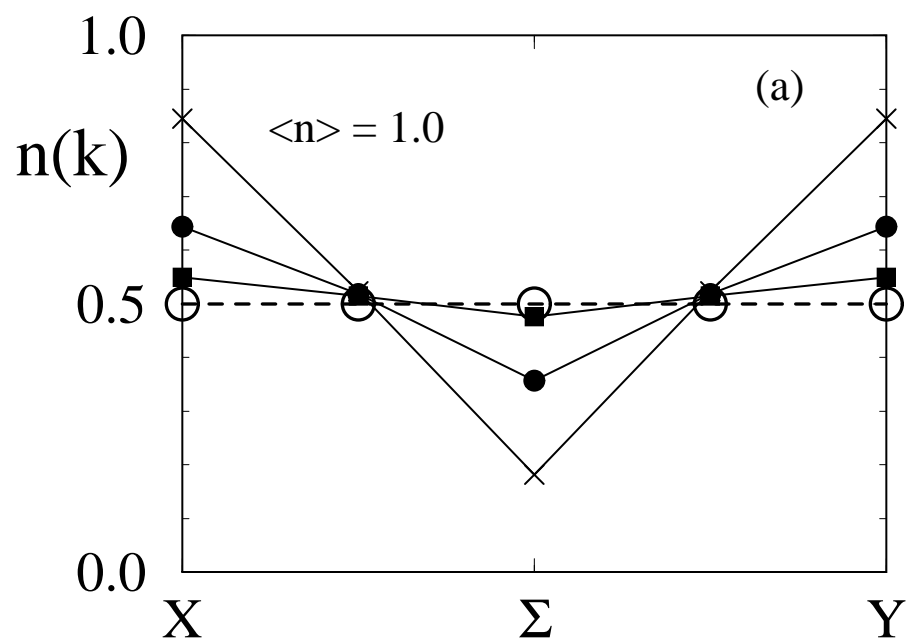


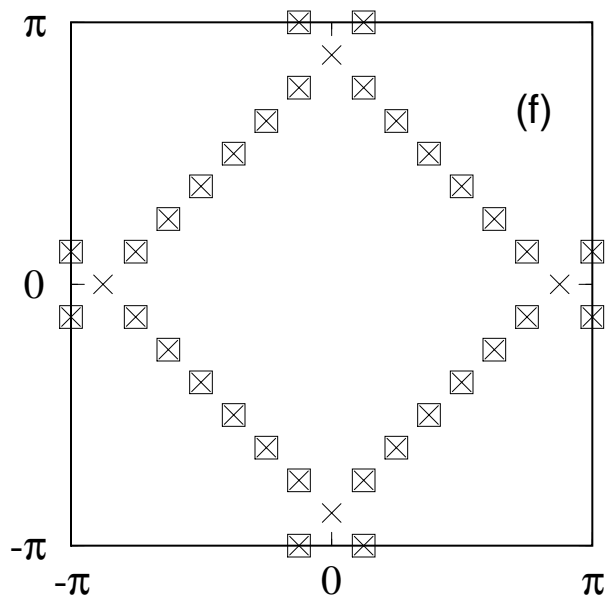
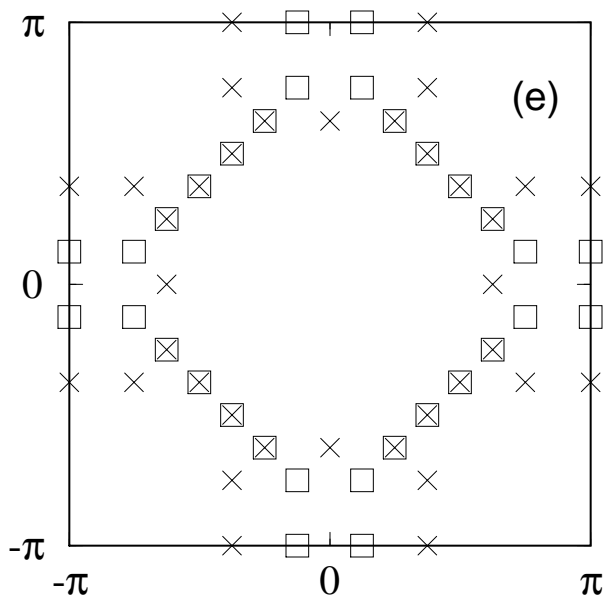
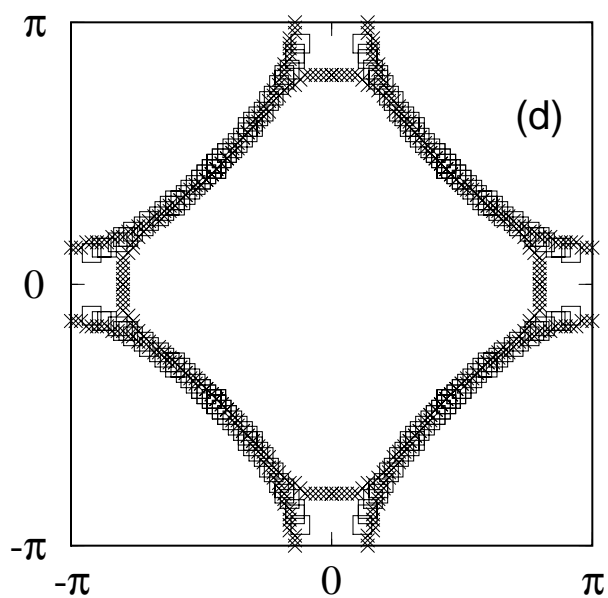
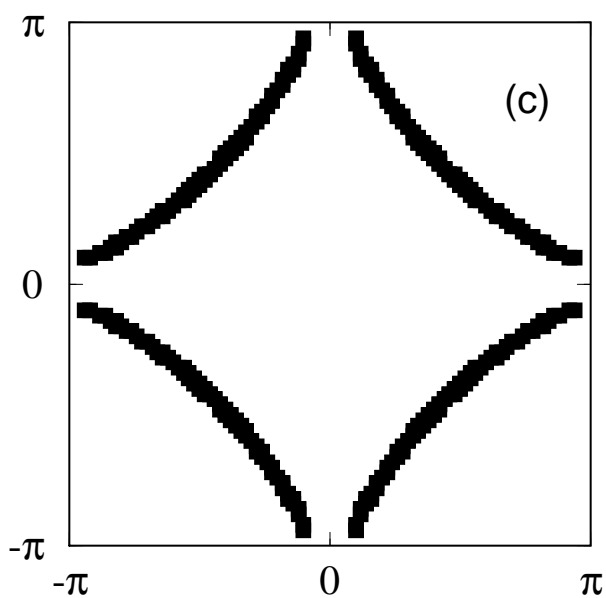
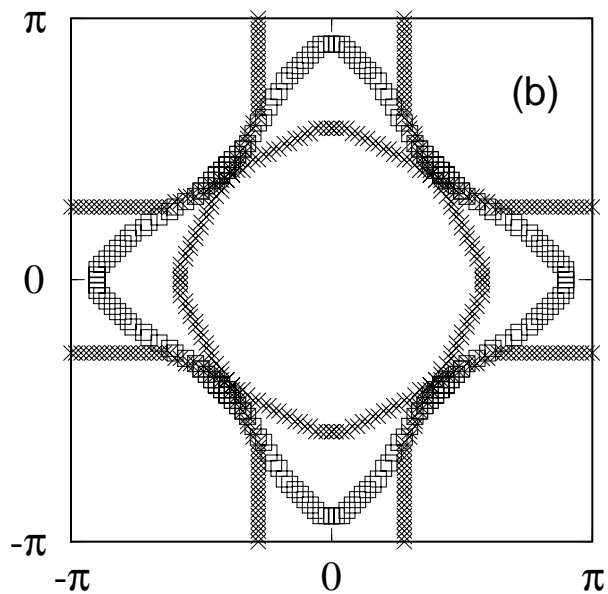
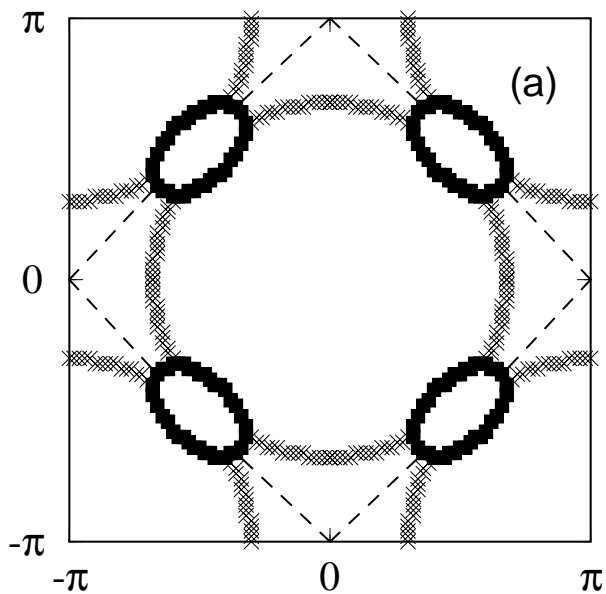






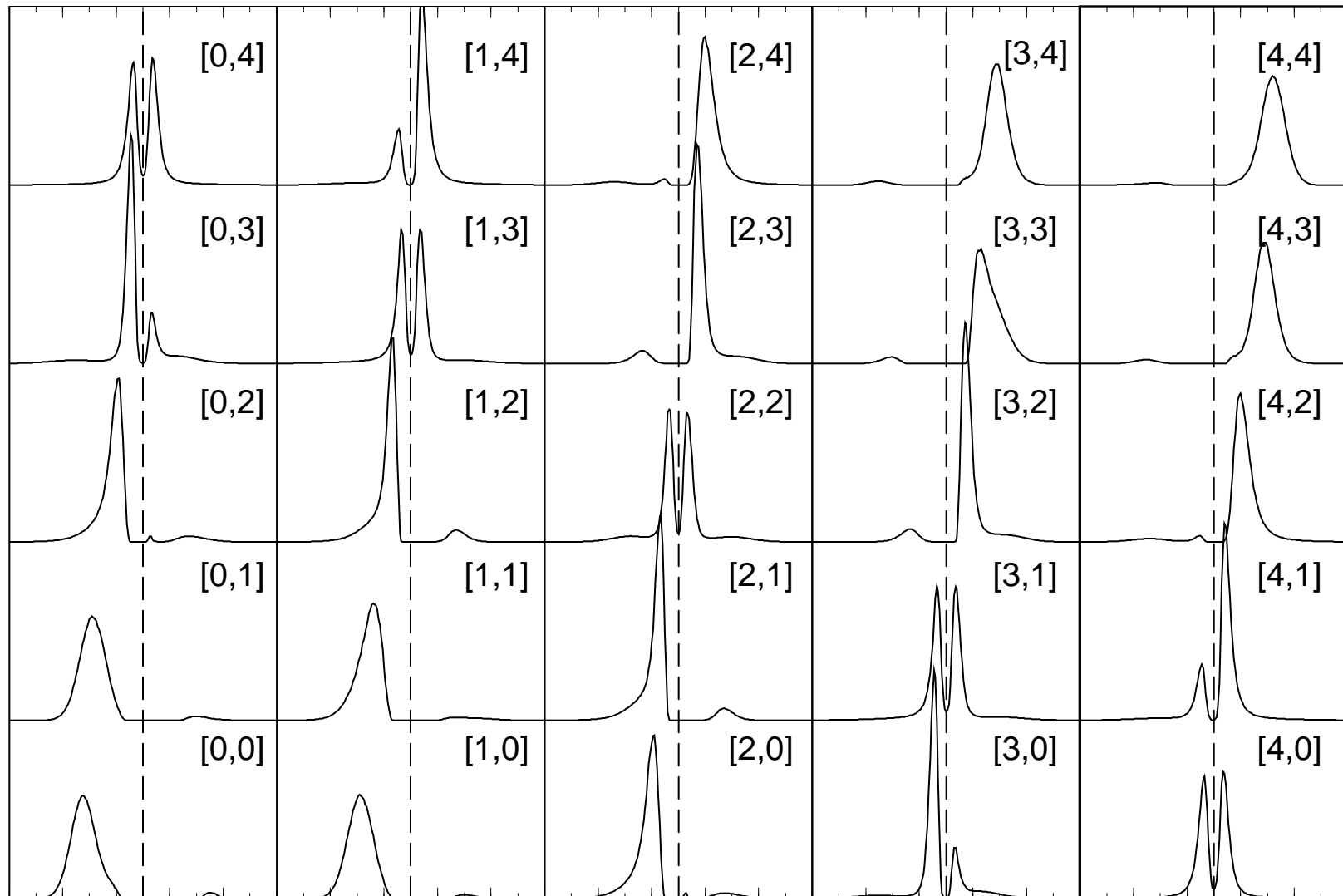
$8 \times 8$ ,  $\beta t = 4$ ,  $t' = -0.2$





$8 \times 8$ ,  $U/t=4$ ,  $\beta t=6$ ,  $\langle n \rangle=1.0$ ,  $t'=0.0$ ,  $\mu=0.0$

(a)

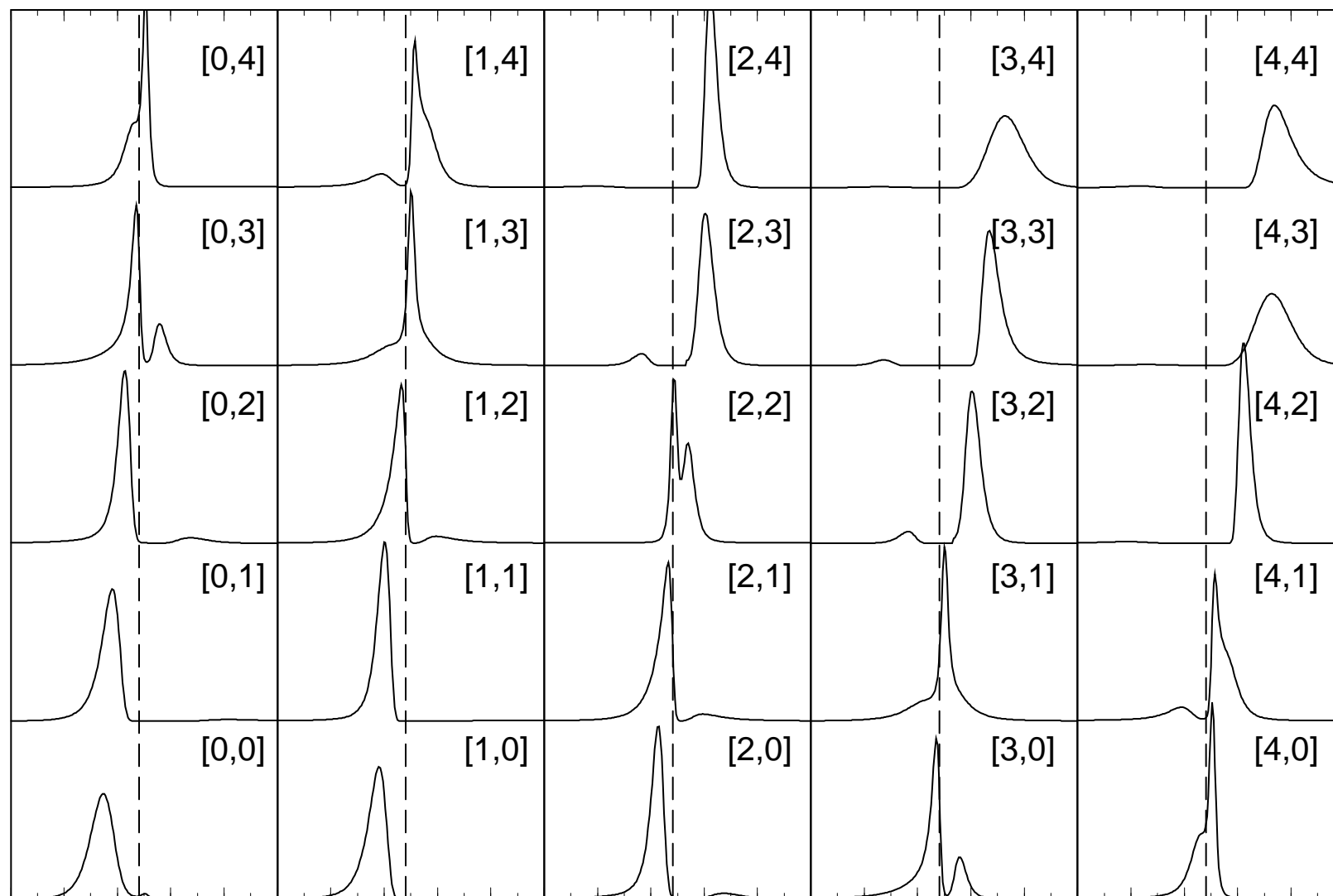


$\text{Max } \omega = 8.0$

$\text{Max } A(\omega) = 0.7$

$8 \times 8$ ,  $U/t=4$ ,  $\beta t=6$ ,  $\langle n \rangle=1.0$ ,  $t'=-0.2$ ,  $\mu=-0.37$

(b)

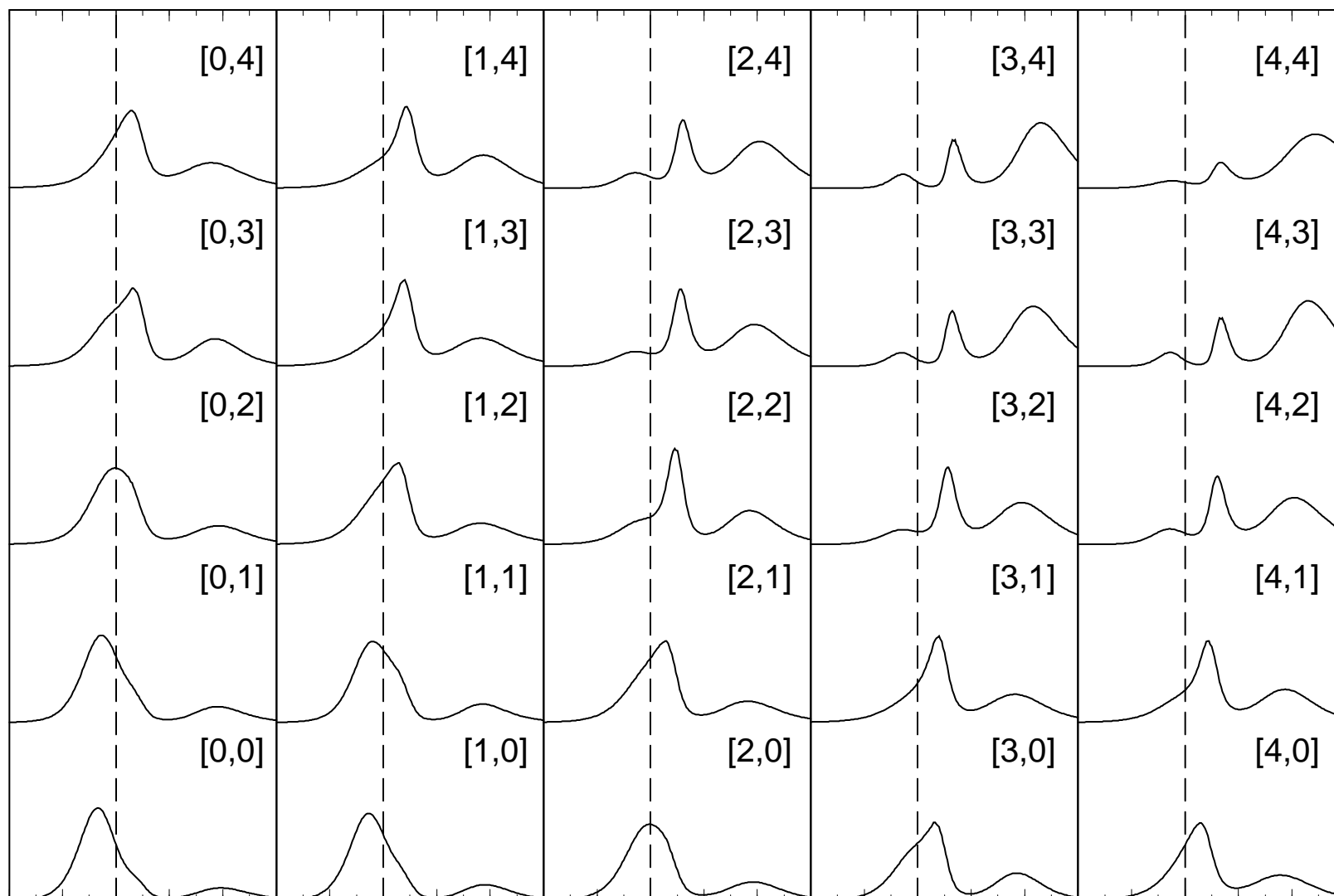


$\text{Max } \omega = 8.0$

$\text{Max } A(\omega) = 0.7$

$8 \times 8$ ,  $U/t=8$ ,  $\beta t=2$ ,  $\langle n \rangle=0.9$ ,  $t'=-0.2$ ,  $\mu=-2.0$

(c)



$\text{Max } \omega = 10.0$

$\text{Max } A(\omega) = 0.4$

